DOI: 10.1002/asia.200700193

Silver(I) Double and Multiple Salts Containing the 1,3-Butadiynediide Dianion: Coordination Diversity and Assembly with the Supramolecular Synthon $Ag_4{\subset}C{\equiv}C{-}C{\equiv}C{\supset}Ag_4$

Liang Zhao,[a] Miao Du,[b] and Thomas C. W. Mak*[a]

Dedicated to Professor Qian-Er Zhang on the occasion of his 79th birthday

Abstract: A series of 13 silver(I) double and multiple salts containing 1,3-butadiynediide, C_4^{2-}, were synthesized by dissolving the silver carbide Ag_2C_4 in a concentrated aqueous solution of one or more of the silver salts $AgNO_3$, $AgCF_3CO_2$, $AgC_2F_5CO_2$, AgF, $AgBF_4$, and $AgPF_6$. The 1,3-butadiynediide anion invariably adopts a μ_4,μ_4 coordination mode in these compounds, which indicates that the $Ag_4{\subset}C{\equiv}C{-}C{\equiv}C{\supset}Ag_4$ moiety can be used as a new type of metalloligand supramolecular synthon for the construction of coordination networks. Fine-tuning with various ancillary anionic ligands caused the Ag_4 aggregate at each ethynide terminus to adopt a butterfly-shaped, planar, or barblike configuration, within which the silver–ethynide interactions can be classified into three types: σ, π, and mixed (σ,π). The effect of coexisting nitrile ligands and quaternary ammonium salts on supramolecular assembly with the above synthon was also explored. The hydrolysis of PF_6^- and BF_4^- led to the formation of the quadruple salt $Ag_2C_4{\cdot}4\,AgNO_3{\cdot}AgPF_2O_2{\cdot}Ag_3PO_4$ and a novel $(F)_2(H_2O)_{18}$ hydrogen-bonded tape in the triple salt $Ag_2C_4{\cdot}2\,AgF{\cdot}10\,AgC_2F_5CO_2{\cdot}CH_3CN{\cdot}12\,H_2O$, respectively. The largest silver–ethynide cluster aggregate described to date, $(C_4)_3@Ag_{18}$, occurs in $3\,Ag_2C_4{\cdot}12\,AgC_2F_5CO_2{\cdot}5[(BnMe_3N)C_2F_5CO_2]{\cdot}4\,H_2O$ (Bn = benzyl).

Keywords: argentophilicity · carbides · coordination modes · silver · supramolecular synthons

Introduction

Metal–polyyne complexes are of current interest, as their linear coordination geometry and π unsaturation make them useful building blocks for rigid-rod molecular wires,[1] which have potential applications as electrical conductors,[2] light-emitting diodes,[3] and nonlinear optical materials.[4] Furthermore, the photoluminescence properties of metal–polyyne complexes have been under intense investigation by several research groups.[5] The terminal ethynide moieties in a polyyne ligand not only act as good σ donors and weak π acceptors to form a large variety of linear metal–alkynyl complexes,[6] but they can also function as good π donors through p_π–d_π overlap with metal atoms to produce a multitude of cluster complexes and multinuclear aggregates.[7,8]

Although the first silver carbide prepared, silver ethynediide (Ag_2C_2), has been known to be a highly explosive material for one and a half centuries,[9] its higher homologues $Ag{-}(C{\equiv}C)_n{-}Ag$ ($n \geq 2$) have seldom been synthesized and are poorly characterized. Hunsmann reported in 1950 that the treatment of 1,6-dichloro-1,3,5-hexatriyne ($Cl{-}C{\equiv}C{-}C{\equiv}C{-}C{\equiv}C{-}Cl$) with $AgNO_3$ in concentrated NH_4OH solution yielded a precipitate, which, however, was not characterized further as a result of its readily explosive nature.[10] Recently, we synthesized crude Ag_2C_4, which is insoluble in most solvents and highly explosive in the dry state when subjected to heating (over 138 °C) or mechanical shock.[11] Raman spectra showed that a typical carbon–carbon triple bond exists in the structure of this polymeric compound. In two structurally related double salts, $Ag_2C_4{\cdot}6\,AgNO_3{\cdot}n\,H_2O$ (n = 2, 3), the $^-C{\equiv}C{-}C{\equiv}C^-$ dianion adopts an unprecedented

[a] L. Zhao, Prof. Dr. T. C. W. Mak
Department of Chemistry
The Chinese University of Hong Kong
Shatin, New Territories, Hong Kong (China)
Fax: (+852) 260-3-5057
E-mail: tcwmak@cuhk.edu.hk

[b] Prof. Dr. M. Du
College of Chemistry and Life Science
Tianjin Normal University, Tianjin (China)

Supporting information for this article is available on the WWW under http://www.chemasianj.org or from the author.

μ_8 coordination mode, with each terminus capped by a butterfly-shaped Ag_4 basket.[11] Moreover, the invariable appearance of this μ_4,μ_4 mode indicates that the $Ag_4{\subset}C{\equiv}C{-}C{\equiv}C{\supset}Ag_4$ moiety may be perceived as a new kind of supramolecular synthon[12] of the metalloligand type[13] for the assembly of coordination networks. As an extension of our studies in this area, we report a series of 13 double and multiple silver salts containing C_4^{2-} and thus provide further insight as to how other coexisting anionic and/or neutral ligands may influence the coordination environment of C_4^{2-}. Our results also establish the general utility of the supramolecular synthon $Ag_4{\subset}C{\equiv}C{-}C{\equiv}C{\supset}Ag_4$ in the construction of multidimensional coordination networks.

Results and Discussion

In our previous synthesis of Ag_2C_4, hexachloro-1,3-butadiene (C_4Cl_6) was treated with *n*BuLi to yield the intermediate compound Li_2C_4[14] through the Fritsch–Buttenberg–Wiechell rearrangement.[15] Thus, half of the silver ions were precipitated as AgCl, which needed to be removed with a concentrated solution of ammonia to give relatively pure silver 1,3-butadiynediide (Ag_2C_4). In the present study, we treated 1,4-bis(trimethylsilyl)-1,3-butadiyne with *n*BuLi and, subsequently, with $AgNO_3$ to produce Ag_2C_4 as a light-gray powder in higher yield. In subsequent synthetic procedures, a concentrated aqueous solution of one or more silver salts was used to dissolve Ag_2C_4 through the formation of $C_4@Ag_8$ moieties consolidated by argentophilic interactions.[16] When $AgPF_6$ was added to an aqueous solution of Ag_2C_4 and $AgNO_3$, the PF_6^- anion was found to undergo hydrolysis to yield $PF_2O_2^-$ and PO_4^{3-}, and we thus isolated the second quadruple salt known to date. A series of 2D and 3D coordination networks based on the $Ag_4{\subset}C{\equiv}C{-}C{\equiv}C{\supset}Ag_4$ supramolecular synthon were obtained through the employment of two perfluorocarboxylate ligands, $CF_3CO_2^-$ and $C_2F_5CO_2^-$, with the option of adding ancillary nitrile ligands RCN (R = Me, Et, *tert*-butyl). The introduction of quaternary ammonium salts as structure-modification agents resulted in lower-dimensional coordination networks.

Abstract in Chinese:

通过将银的碳化物 Ag_2C_4 溶解于一系列银盐的水溶液，包括硝酸银、三氟乙酸银、五氟丙酸银加上氟化银、四氟硼酸银和六氟磷酸银，我们合成十三个含有 1，3-丁二炔二负离子的一价银的双盐和多重复盐。其中，1，3-丁二炔二负离子的μ_4,μ_4-配位模式稳定地出现在这些化合物的结构中，表明 $Ag_4{\subset}C{\equiv}C{-}C{\equiv}C{\supset}Ag_4$ 可以作为一种新的金属-配体类型的超分子合成子用于构建配位网络。进一步的，通过采用不同的辅助阴离子配体，可以调整末端炔基负离子周围的四核银聚集体的构型，从而形成蝶形、平面型或鱼钩状结构，其中的银–炔基作用可以分成三类：σ、π 和混合 (σ, π) 。此外，我们也研究了共存的腈类以及季铵盐类配体对上述合成子的超分子组装的影响。值得注意的是，通过六氟磷酸根和四氟硼酸根的水解，我们获得了第二个银的四盐化合物 $Ag_2C_4\cdot 4AgNO_3\cdot AgPF_2O_2\cdot Ag_3PO_4$，并于 $Ag_2C_4\cdot 2AgF\cdot 10AgC_2F_5CO_2\cdot CH_3CN\cdot 12H_2O$ 中找到一种新奇的带状 $(F)_2(H_2O)_{18}$ 氢键联系结构。迄今最大的银–炔基簇 $(C_4)_3@Ag_{18}$ 也于 $3Ag_2C_4\cdot 12AgC_2F_5CO_2\cdot 5[(BnMe_3N)C_2F_5CO_2]\cdot 4H_2O$ 中被发现。

$2\,Ag_2C_4{\cdot}2\,AgF{\cdot}6\,AgNO_3{\cdot}H_2O$ (1)

The crystal structure of the triple salt $2\,Ag_2C_4{\cdot}2\,AgF{\cdot}6\,AgNO_3{\cdot}H_2O$ (**1**) contains two different types of $[Ag_4C_4Ag_4]$ aggregate, as shown in Figure 1a. The first C_4^{2-} dianion (C2≡C1−C1A≡C2A) is located at an inversion center, with each terminus surrounded by a butterfly-shaped Ag_4 basket. The resulting $[Ag_4C_4Ag_4]$ aggregate has a quasi-C_{2h} axis with a mirror plane that passes through the C_4 chain and four silver atoms (Ag4, Ag6, Ag4A, and Ag6A). The Ag4 atom is π-bonded to the ethynide terminal C1≡C2 bond with Ag4−C1 = 2.667(7) Å. This distance is longer than the other Ag−C distances, which range from 2.128(5) to 2.519(7) Å. Another C_4^{2-} dianion, C4≡C3−C3B≡C4B, is located on a C_2 axis with each ethynide terminus capped by a barblike Ag_4 basket. The C_4 chain lies perpendicular to the plane that passes through three silver atoms (Ag4, Ag5, and Ag6A), with Ag−C distances of 2.347(6)–2.508(6) Å, and points toward the silver atom Ag3 at a C3−C4−Ag3 angle of 178.8(5)°. The C4−Ag3 distance of 2.067(6) Å is the shortest reported for 1,3-butadiyne-1,4-diyl–silver complexes.[11,17] This unusual barblike bonding mode of the ethynide moiety was once reported for copper–alkyl ethynide complexes.[18]

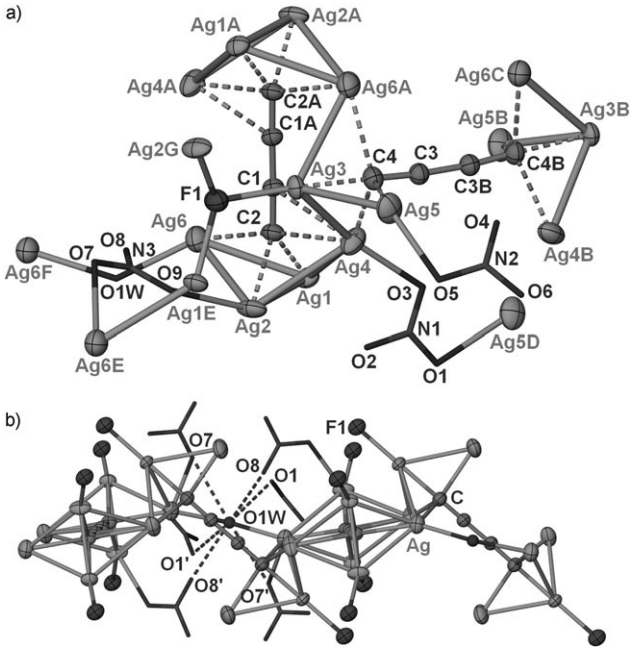

Figure 1. a) Atom labeling (50% thermal ellipsoids) and coordination modes of the anionic ligands in $2\,Ag_2C_4{\cdot}2\,AgF{\cdot}6\,AgNO_3{\cdot}H_2O$ (**1**). Symmetry codes: A: $^1/_2-x$, $1^1/_2-y$, $1-z$; B: $1-x$, y, $1^1/_2-z$; C: $^1/_2+x$, $1^1/_2-y$, $^1/_2+z$; D: x, $1-y$, $z-^1/_2$; E: x, $1-y$, $^1/_2+z$; F: $-x$, y, $^1/_2-z$; G: $^1/_2-x$, $^1/_2+y$, $1^1/_2-z$. Selected bond lengths and distances (Å): C1−C2 1.234(8), C3−C4 1.229(8), Ag···Ag 2.782(1)–3.338(6). b) Coordination column in **1** formed through the fusion of two types of $[Ag_4C_4Ag_4]$ aggregates. The distorted-octahedral hydrogen-bonding environment of the bridging aqua ligand O1W, which lies on a crystallographic C_2 axis, is indicated by dashed lines. Selected distances (Å): O1W···O1 2.793, O1W···O7 2.912, O1W···O8 2.796.

As shown in Figure 1b, two C_4 chains in **1** are perpendicular to one another (90.4°), and the aforementioned two $[Ag_4C_4Ag_4]$ aggregates coalesce by sharing two silver atoms of the type Ag4 and Ag6 to generate a coordination column along the [101] direction. Hydrogen bonding between the disordered hydrogen atoms of the aqua ligand O1W, which is located on a crystallographic C_2 axis, and six oxygen atoms of nitrate groups plays a role in the stabilization of the columnar structure. These coordination columns are arranged in a pseudohexagonal array and are further connected by two μ_2 nitrate groups (N1 and N3) and one μ_3 fluoride ligand (F1) to form a structurally robust 3D coordination network (Figure 2). Notably, the sum of three Ag–F–Ag angles for this μ_3 fluoride ligand is 337.7°, which indicates an unusual trigonal-pyramidal coordination mode that differs from the planar μ_3 mode in some reported silver complexes.[19]

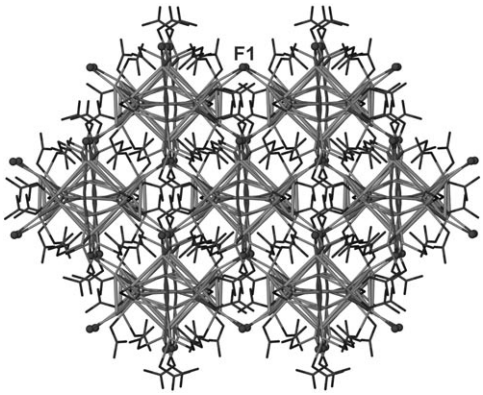

Figure 2. 3D coordination network in **1** viewed along the [101] direction.

$Ag_2C_4{\cdot}4\,AgNO_3{\cdot}AgPF_2O_2{\cdot}Ag_3PO_4$ (2)

To increase the concentration of the silver ions required to dissolve Ag_2C_4 and to adjust the molar ratio of the cation (Ag^+) and anions (C_4^{2-} and NO_3^-), we initially introduced $AgPF_6$ as an additive because of its high solubility in water and the poor coordination ability of the hexafluorophosphate anion. However, PF_6^- underwent unexpected hydrolysis to yield both $PF_2O_2^-$ and PO_4^{3-} anions. It is well-known that the hydrolysis of hexafluorophosphate (PF_6^-) generates the difluorophosphate anion $PF_2O_2^-$, which occurs in a number of crystal structures.[20] There are, however, only a few instances in which crystalline compounds containing PO_4^{3-} are generated by the complete hydrolysis of hexafluorophosphate.[20b,21] Two tetrahedral oxophosphate ligands coexist in the crystal structure of $Ag_2C_4{\cdot}4\,AgNO_3{\cdot}AgPF_2O_2{\cdot}Ag_3PO_4$ (**2**; Figure 3a). The experimental bond lengths at the two phosphorus centers (P1 and P2) are listed in Table 1. Relative to the bond lengths at P2 (1.486(11)–1.562(11) Å), there is one much shorter bond of 1.437(13) Å and one much longer bond of 1.604(11) Å in the oxophosphate ligand P1, which indicates that these two phosphate ligands should be differentiated. If the charge-

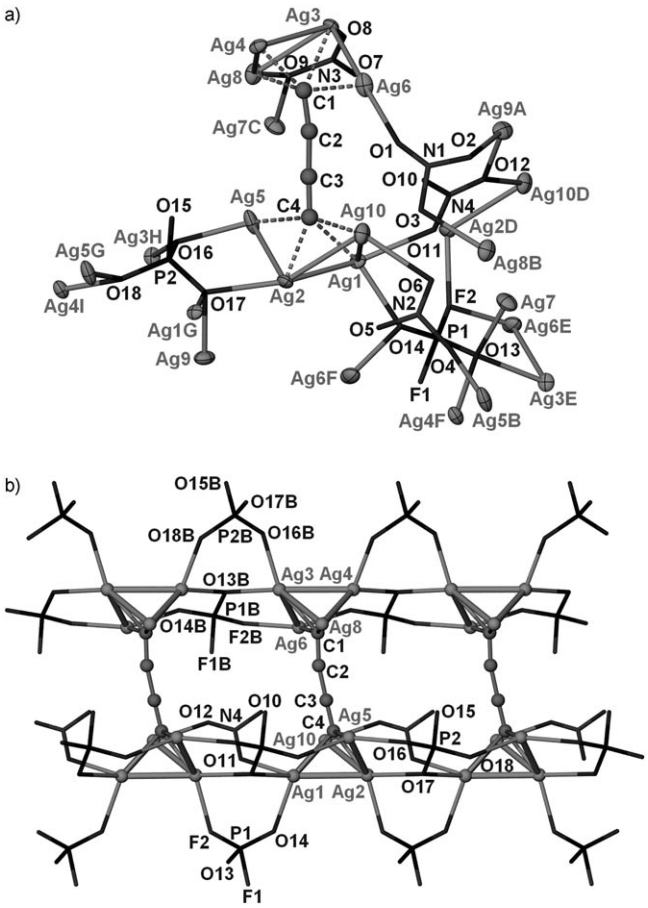

Figure 3. a) Atom labeling (50% thermal ellipsoids) and coordination modes of the anionic ligands in $Ag_2C_4{\cdot}4\,AgNO_3{\cdot}AgPF_2O_2{\cdot}Ag_3PO_4$ (**2**). Symmetry codes: A: $1-x$, $y-\frac{1}{2}$, $1-z$; B: x, y, $1+z$; C: x, y, $z-1$; D: $x-1$, y, z; E: $-x$, $\frac{1}{2}+y$, $1-z$; F: $1-x$, $\frac{1}{2}+y$, $1-z$; G: $1+x$, y, z; H: $1-x$, $\frac{1}{2}+y$, $-z$; I: $2-x$, $\frac{1}{2}+y$, $-z$. Selected bond lengths and distances (Å): C1–C2 1.25(3), C3–C4 1.22(2), Ag···Ag 2.826(2)–3.001(2). b) Coordination column in **2** along the *a* direction connected by $PF_2O_2^-$ and PO_4^{3-} on one side and by these two groups plus the nitrate ligand N4 on the other side.

Table 1. Ligation environments and bond lengths at the two phosphorus centers (P1 and P2) in complex **2**. (Symmetry codes are given in Figure 3).

Ligand	Atom (X)	P–X [Å]	X–Ag [Å]	Mean X–Ag [Å]
P1	F1	1.604(11)		
	F2	1.549(11)	Ag2D 2.297(13)	2.300
			Ag6E 2.302(12)	
	O13	1.481(15)	Ag3E 2.404(16)	2.405
			Ag4F 2.506(14)	
			Ag7 2.31(2)	
	O14	1.437(13)	Ag1 2.363(13)	2.357
			Ag6F 2.351(14)	
P2	O15	1.517(19)		
	O16	1.486(11)	Ag3H 2.287(13)	2.328
			Ag5 2.368(11)	
	O17	1.559(9)	Ag1G 2.429(8)	2.379
			Ag2 2.436(8)	
			Ag9 2.271(10)	
	O18	1.562(11)	Ag4I 2.204(11)	2.324
			Ag5G 2.443(11)	

balance requirement and the process for the hydrolysis of PF_6^- are taken into account, the following combinations of these two anionic ligands are possible: 1) $H_2PO_4^- + PO_4^{3-}$, 2) $HPO_4^{2-} + PFO_3^{2-}$, or 3) $PF_2O_2^- + PO_4^{3-}$. The first combination is excluded because in that case one protonated oxygen atom of $H_2PO_4^-$ would bond with at least two silver atoms to result in the μ_7-η^2,η^2,η^3 bonding mode for both phosphate ligands. There is no precedent for such an arrangement in the reported metal complexes of $H_2PO_4^-$ (see the Supporting Information).[22] Although PFO_3^{2-} is also a plausible intermediate in the hydrolysis of PF_6^-, only a few crystalline solids contain this anionic ligand derived from hexafluorophosphate.[23] We compared the P–X (X = O or F) bond distances in **2** with those in reported complexes that contain HPO_4^{2-}, PFO_3^{2-}, and $PF_2O_2^-$,[24] and reached the conclusion that the anions $PF_2O_2^-$ and PO_4^{3-} coexist in complex **2**. This is the second silver(I) quadruple salt that contains four different anions (C_4^{2-}, NO_3^-, $PF_2O_2^-$, and PO_4^{3-}). The first such salt to be described was $2Ag_2C_2 \cdot 3AgCN \cdot 15AgCF_3CO_2 \cdot 2AgBF_4 \cdot 9H_2O$.[25] Among the limited number of silver phosphate complexes that have been subjected to crystal-structure analysis,[26] this is the first in which a μ_7-η^2,η^2,η^3 coordination mode has been observed for PO_4^{3-}. Furthermore, the μ_7-η^2,η^2,η^3 coordination mode of $PF_2O_2^-$ corresponds to the highest ligation number known for this ligand.[20,27]

Each terminus of the C_4^{2-} dianion is encapsulated in a butterfly-shaped Ag_4 basket with silver–ethynide interactions that range from 2.134(16) to 2.401(16) Å. These quasi-C_{2h} [$Ag_4C_4Ag_4$] aggregates are connected by $PF_2O_2^-$ and PO_4^{3-} at one end and by their symmetry equivalents plus one nitrate group (N4) at the other end to form a coordination column along the *a* direction (Figure 3b). The linkage of adjacent columns arranged in a hexagonal array normal to [100] through the remaining three independent nitrate groups (N1, N2, and N3) in μ_3-O,O′,O″, μ_2-O,O′, and μ_3-O,O,O′ modes, respectively, with the aid of the remaining bonding sites of the ligands centered at P1, P2, and N4, then generates a 3D coordination network (Figure 4).

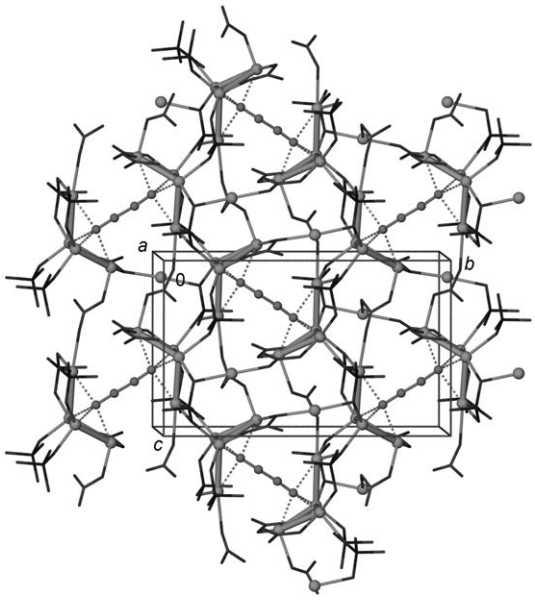

Figure 4. Pseudohexagonal array of coordination columns in **2** linked by nitrate and phosphate groups to yield a 3D coordination network.

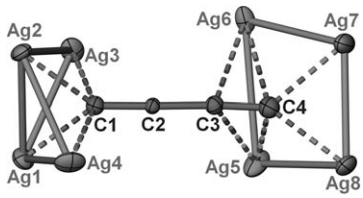

Figure 5. Atom labeling (50% thermal ellipsoids) and unsymmetrical coordination mode of C_4^{2-} in $Ag_2C_4 \cdot 6AgCF_3CO_2 \cdot 7H_2O$ (**3**). Other ligands are omitted for clarity. Selected bond lengths and distances (Å): C1–C2 1.27(3), C3–C4 1.21(3), Ag···Ag 2.718(3)–3.250(5).

$Ag_2C_4 \cdot 6AgCF_3CO_2 \cdot 7H_2O$ (3)

Although the μ_8 bonding mode of C_4^{2-} with a butterfly-shaped Ag_4 basket at each end is dominant in nitrate complexes of Ag_2C_4, it is believed that diverse silver aggregates can be obtained by varying the anionic ligands. The use of silver trifluoroacetate in place of silver nitrate in the crystallization step led to the formation of $Ag_2C_4 \cdot 6AgCF_3CO_2 \cdot 7H_2O$ (**3**), in which one terminal ethynide, C1≡C2, bonds to a commonly observed butterfly-shaped Ag_4 basket through silver–ethynide interactions in the range 2.156(19) to 2.360(19) Å, and the other, C3≡C4, to a planar Ag_4 segment through a μ_4-$\eta^1,\eta^1,\eta^2,\eta^2$ bonding mode (Figure 5). Although such a coordination mode has been reported for a terminal ethynide moiety with a planar M_4 aggregate in transition-metal complexes,[28] in such cases the C–C≡C bond angles are mostly bent, in contrast to the nearly linear bond angle of 173(2)° in **3**. The C_4 chain points slantwise at an angle of 43° to the mean plane defined by Ag5, Ag6, Ag7, and Ag8.

Owing to this unusual ligation mode of C_4^{2-}, adjacent [$Ag_4C_4Ag_4$] aggregates can be connected mutually by the linkage of two μ_3-O,O′,O′ trifluoroacetate groups (O7–O8 and O9–O10) and one aqua ligand (O6W) to generate a 2_1 helix along the *a* direction (Figure 6a). These infinite helical coordination columns are arranged in a hexagonal array viewed along [100] and further bridged by the other two μ_3-O,O′,O′ trifluoroacetate groups (O5–O6 and O11–O12) to yield a 3D coordination network (Figure 6b).

$Ag_2C_4 \cdot 7AgCF_3CO_2 \cdot CH_3CN \cdot 4H_2O$ (4)

Unsymmetrical coordination of 1,3-butadiynediide is possible not only through the presence of different Ag_4 configurations at the two termini of the C_4 chain, but also through the variation of σ and π silver–ethynide bonding. In the crystal structure of $Ag_2C_4 \cdot 7AgCF_3CO_2 \cdot CH_3CN \cdot 4H_2O$ (**4**), the ethynide moiety C1≡C2 is bound to a butterfly-shaped

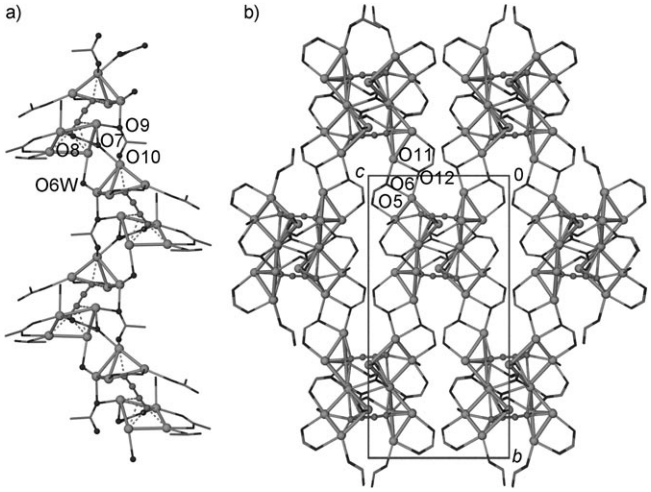

Figure 6. a) Coordination column in **3** with a 2_1 *M*-type (left-handed) axis along [100] formed through the connection of two μ_3 trifluoroacetate groups (O7–O8 and O9–O10) and one aqua ligand (O6W). b) Hexagonal array of helical coordination columns in **3** bridged by trifluoroacetate groups (O5–O6 and O11–O12) through the μ_3-O,O′,O′ bonding mode. All trifluoromethyl moieties of $CF_3CO_2^-$ are omitted for clarity.

Ag_4 basket by σ bonding in the range 2.216(6) to 2.483(7) Å, and C3≡C4 is encapsulated in a similar Ag_4 basket through both σ and π silver–ethynide interactions, with σ bonds in the range 2.214(7) to 2.440(6) Å and a π interaction between Ag5 and C3 at a distance of 2.548(5) Å. Two inversion-related $[Ag_4C_4Ag_4]$ aggregates are connected by a Ag2···Ag2A edge and four μ_3-O,O′,O′ trifluoroacetate groups (of the type O5–O6 and O7–O8) to form a building unit (Figure 7a); such units are further linked by the other trifluoroacetate groups (of the type O9–O10 and O11–O12) along [$\bar{1}$10] to produce a polymeric coordination chain. The linkage of adjacent coordination chains through the external silver atom Ag4, which is bonded to an acetonitrile group and two aqua ligands (O2W and O3W), generates a 2D coordination network parallel to the *ab* plane. This network is further stabilized by four types of hydrogen bonds between adjacent polymeric chains (Figure 7b).

Furthermore, these 2D coordination networks packed along the *c* direction are bridged by a series of μ_3-O,O′,O′ trifluoroacetate groups of the type O1–O2 and O3–O4 to yield a 3D coordination network, in which the orientations of polymeric chains of successive layers follow the order A[$\bar{1}$10] B[110] A[$\bar{1}$10] B[110]… (Figure 8).

$Ag_2C_4{\cdot}10\,AgCF_3CO_2{\cdot}2\,[(Et_4N)CF_3CO_2]{\cdot}4\,(CH_3)_3CCN$ (5)

In the crystal structure of $Ag_2C_4{\cdot}10\,AgCF_3CO_2{\cdot}2\,[(Et_4N)CF_3CO_2]{\cdot}4\,(CH_3)_3CCN$ (**5**), the centrosymmetric C_4^{2-} dianion is located inside a metallocarboxylate ring comprising two terminal butterfly-shaped Ag_4 baskets and two inversion-related trifluoroacetate groups of the type O11–O12 (Figure 9a). The Ag–O bonds to the trifluoroacetate groups in the ring are markedly shorter (2.245(9)–2.250(9) Å) than the Ag–O bonds for the remaining five tri-

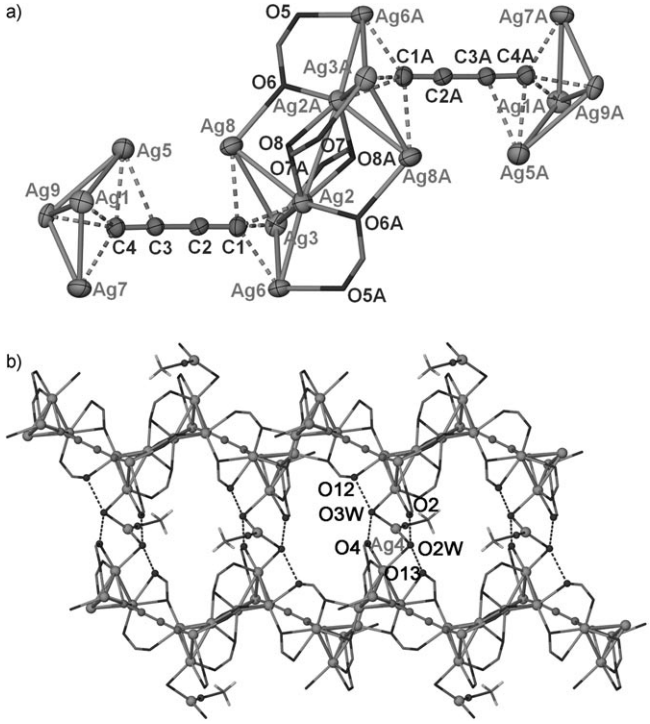

Figure 7. a) Atom labeling (50% thermal ellipsoids) of a building unit bridged by four μ_3-O,O′,O′ trifluoroacetate groups in $Ag_2C_4{\cdot}7\,AgCF_3CO_2{\cdot}CH_3CN{\cdot}4\,H_2O$ (**4**). All CF_3 moieties of trifluoroacetate groups and other ligands are omitted for clarity. Symmetry code: A: $^1/_2-x$, $1^1/_2-y$, $1-z$. Selected bond lengths and distances (Å): C1–C2 1.214(8), C3–C4 1.230(8), Ag···Ag 2.725(3)–3.308(1). b) 2D coordination network formed through the linkage of adjacent polymeric chains by an O3W–Ag4–O2W moiety and four hydrogen bonds (Å): O2W···O2 2.794, O2W···O13 2.753, O3W···O4 2.836, O3W···O12 2.893. All fluorine atoms are omitted for clarity.

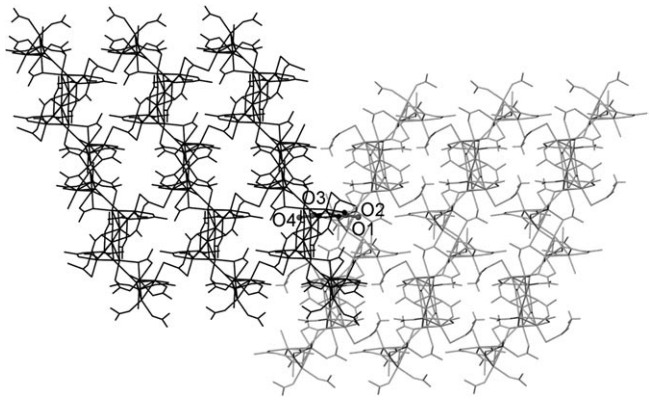

Figure 8. The packing of 2D coordination networks in **4** along the *c* direction and linkage by two μ_3-O,O′,O′ trifluoroacetate groups (O1–O2 and O3–O4) generates a 3D coordination network. Different 2D coordination networks composed of polymeric chains along A[110] and B[110] are indicated in black and gray, respectively.

fluoroacetate groups in the structure (2.327(7)–2.580(7) Å). Three trifluoroacetate groups (O1–O2, O7–O8, and O9–O10) each span an Ag···Ag edge through the μ_2-O,O′ mode, whereas the other two trifluoroacetate groups (O3–O4 and

CHEMISTRY
AN ASIAN JOURNAL

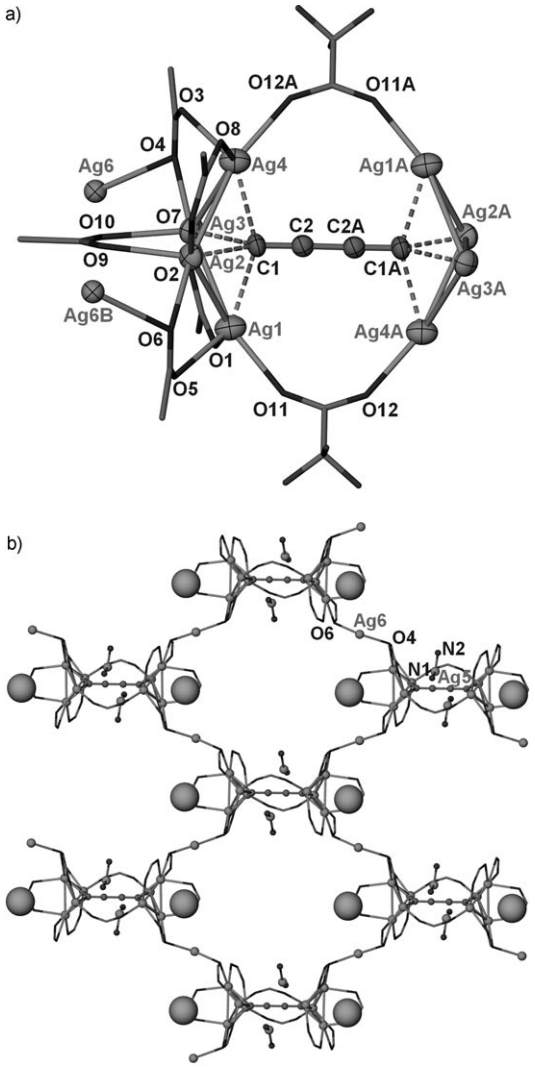

Figure 9. a) Atom labeling (50% thermal ellipsoids) in $Ag_2C_4{\cdot}10\,AgCF_3CO_2{\cdot}2\,[(Et_4N)CF_3CO_2]{\cdot}4\,(CH_3)_3CCN$ (**5**), which contains a metallacycle formed by two terminal Ag_4 baskets and two trifluoroacetate groups. Some fluorine atoms and other groups are omitted for clarity. Symmetry codes: A: $1-x$, $1-y$, $1-z$; B: $^1/_2-x$, $y-^1/_2$, $^1/_2-z$. Selected bond lengths and distances (Å): C1–C2 1.223(9), Ag···Ag 2.830(1)–2.923(1). b) Rosette metallacycle in **5** generated through the linkage of metallocarboxylate rings by the external silver atom Ag6 and two trifluoroacetate groups (O3–O4 and O5–O6). The tetraethylammonium cation (Et_4N^+) is denoted by a large gray sphere.

O5–O6) bridge the $[Ag_4C_4Ag_4]$ unit and the external silver atom Ag6 through the μ_3-O,O′,O′ mode. Accordingly, the $[Ag_4C_4Ag_4]$ units are interlinked to generate a rosettelike metallacycle, in which the enclosed tetraethylammonium cations (Et_4N^+), which are located above and below the metallacycle, project at two opposite petal positions. Two trimethylacetonitrile ligands are bonded to another external silver atom, Ag5, at each of the remaining petal positions, and one of these ligands protrudes into the macrometallacycle (Figure 9b). The dihedral angle between this macrocycle and the aforementioned metallocarboxylate ring is 71.7°. The tiling of the rosette metallacycles yields a 2D coordination network parallel to the $(10\bar{1})$ plane.

Such 2D networks are then packed along the $[\bar{1}01]$ direction. Every $[Ag_4C_4Ag_4]$ unit in the upper network lies exactly above the center of a rosette metallacycle of the network below. This arrangement results in a series of voids between adjacent networks to accommodate the tetraethylammonium cations (Figure 10). Adjacent 2D networks are separated by 12.75 Å.

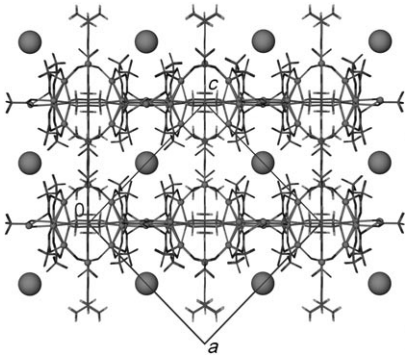

Figure 10. Packing view of 2D coordination networks in **5** viewed along the *b* direction. Each gray sphere represents a tetraethylammonium cation.

$[Ag_{16}(C_4)(C_2F_5CO_2)_{16}(H_2O)_8]{\cdot}2\,(H_3O^+){\cdot}14\,H_2O$ (6)

Yellow blocklike crystals of $[Ag_{16}(C_4)(C_2F_5CO_2)_{16}(H_2O)_8]{\cdot}2\,(H_3O^+){\cdot}14\,H_2O$ (**6**) crystallize in the high-symmetry space group $P4_2/nmc$. The C_4^{2-} carbon-atom chain and the hydronium cation generated under acidic conditions (pH 2–3) are both located on the 4_2 axis. Each terminus of the carbon-atom chain is encircled by three concentric annuli, and the C_4 chain is completely perpendicular to these planar rings (Figure 11a). The square Ag_4 segment that surrounds the ethynide moiety at each terminus constitutes the first annulus, which is bound by the ethynide C1≡C2 through four Ag–C σ bonds of 2.206(12) Å in length to form an unprecedented dumbbell-like $[Ag_4C_4Ag_4]$ aggregate. The second annulus is a 12-membered metallacycle that consists of eight oxygen atoms of four μ_4-O,O,O′,O′ pentafluoropropionate groups and four silver atoms of the type Ag1. In the peripheral environment, the fluorine atoms of eight μ_2-O,O′ pentafluoropropionate groups (of the type O1–O2), each of which spans two inversion-related silver atoms of the type Ag1, together with the four aforementioned μ_4-O,O,O′,O′ pentafluoropropionate groups comprise the four hydrophilic arcs of the third annulus. This dumbbell-like $[Ag_4C_4Ag_4]$ aggregate contains eight $[Ag_2(\mu_2\text{-}C_2F_5CO_2)_2]$ linking units to connect eight dumbbell building blocks with the formation of a robust 3D coordination network (Figure 11b).

A crownlike 12-membered water ring linked by hydrogen bonding between O1W and O2W also surrounds the $[Ag_4C_4Ag_4]$ aggregate (Figure 12a). The remaining water molecules (O3W and O4W) and hydronium cation (O5W) are buried inside a series of infinite channels along the *a* di-

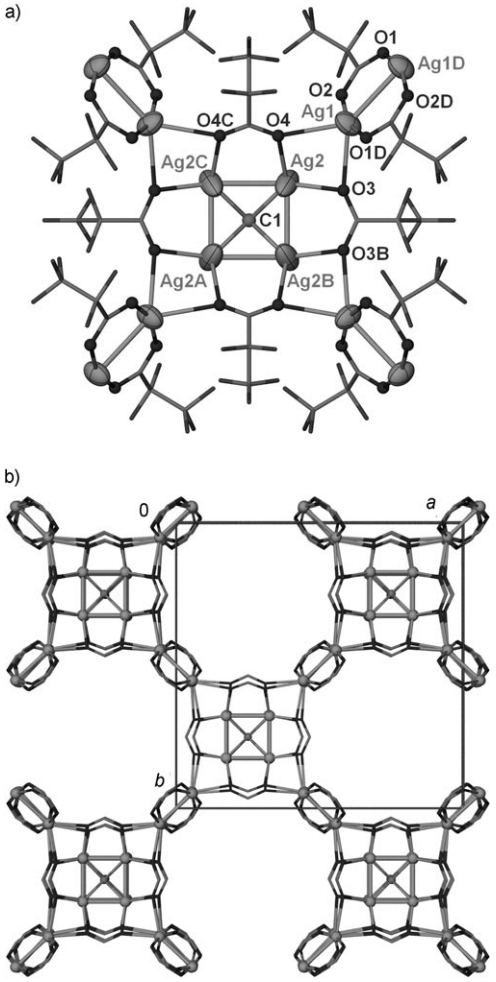

Figure 11. a) Atom labeling (50% thermal ellipsoids) and coordination modes of the terminal ethynide moiety and pentafluoropropionate groups in $[Ag_{16}(C_4)(C_2F_5CO_2)_{16}(H_2O)_8]\cdot 2(H_3O^+)\cdot 14H_2O$ (**6**), viewed along the C_4 carbon chain. Water molecules and hydronium ions are omitted for clarity. Symmetry codes: A: $^1/_2-x$, $1^1/_2-y$, z; B: x, $1^1/_2-y$, z; C: $^1/_2-x$, y, z; D: $1-x$, $1-y$, $1-z$. Selected bond lengths and distances (Å): C1–C2 1.18 (3), Ag···Ag 2.86(2)–3.10(2). b) 3D coordination networks bridged by eight $[Ag_2(\mu_2\text{-}C_2F_5CO_2)_2]$ linking units. All C_2F_5 moieties of $C_2F_5CO_2$ groups and other ligands are omitted for clarity.

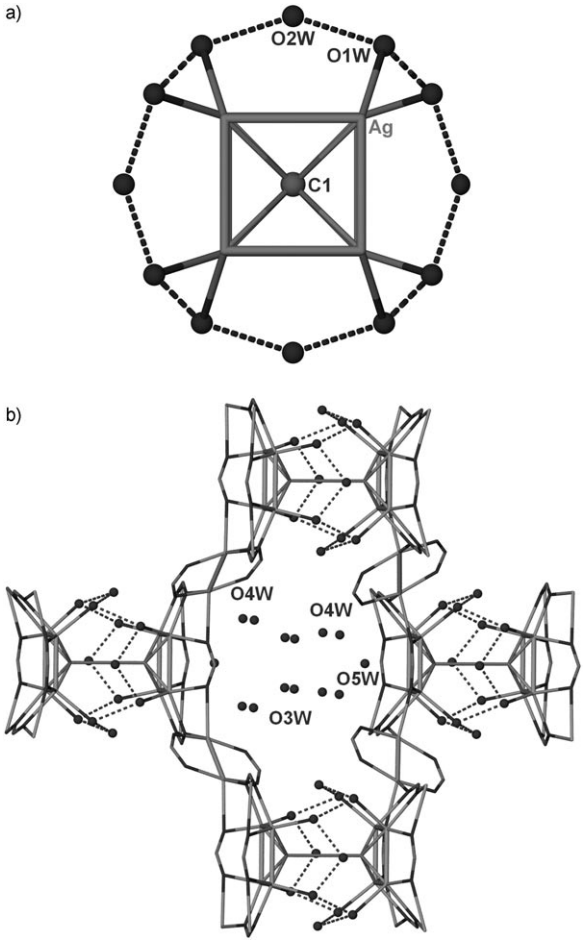

Figure 12. a) Crownlike water ring surrounding the $[Ag_4C_4Ag_4]$ aggregate in **6**. Hydrogen-bond distances (Å): O1W···O2W 2.827, O1W···O1W′ 2.647. b) Infinite channel filled with water molecules along the *a* direction. All C_2F_5 moieties of $C_2F_5CO_2$ groups and other ligands are omitted for clarity.

rection (Figure 12b). Although it is clear that extensive hydrogen bonding exists within each water channel, positional disorder of the oxygen atoms precludes their precise location.

$Ag_2C_4\cdot 16\,AgC_2F_5CO_2\cdot 6\,CH_3CN\cdot 8\,H_2O$ (7)

Upon the addition of acetonitrile to the crystallization medium in the preparation of **6**, the configuration of the Ag_4 aggregate at each 1,3-butadiynediide terminus changes from planar to butterfly-shaped. In the new complex, $Ag_2C_4\cdot 16\,AgC_2F_5CO_2\cdot 6\,CH_3CN\cdot 8\,H_2O$ (**7**), the silver–ethynide interactions lie in the range 2.171(9) to 2.443(9) Å. The butterfly-shaped Ag_4 basket at each terminus is surrounded by three μ_4-O,O,O′,O′ pentafluoropropionate groups (O5–O6, O7–O8, and O11–O12) and two μ_2-O,O′ groups (O9–O10 and O13–O14). The pentafluoropropionate groups in the μ_4 bonding mode are connected to three $[Ag_2(\mu_2\text{-}C_2F_5CO_2)_2]$ bridging units and an external silver atom, Ag8, which is bonded to an acetonitrile group (Figure 13a). The $[Ag_4C_4Ag_4]$ aggregates are connected by bridging units of the type Ag5–Ag6 to yield a (4,4) coordination network parallel to the *bc* plane (Figure 13b), and this network is further linked by the other two axial bridging units of the type Ag7–Ag7 to form a 3D coordination network.

$Ag_2C_4\cdot 2\,AgF\cdot 10\,AgC_2F_5CO_2\cdot CH_3CN\cdot 12\,H_2O$ (8)

The crystal structure of $Ag_2C_4\cdot 2\,AgF\cdot 10\,AgC_2F_5CO_2\cdot CH_3CN\cdot 12\,H_2O$ (**8**) contains two independent C_4^{2-} ligands, each of which is located at an inversion center and enveloped within a closed silver-atom ring (Figure 14a). The first metallacycle, B, can be viewed as an eight-membered ring composed of Ag4, Ag8, Ag9, Ag10, and their inversion-related atoms, with two silver atoms of the type Ag11 attached to it. The eight silver atoms in the ring are almost coplanar

CHEMISTRY
AN ASIAN JOURNAL

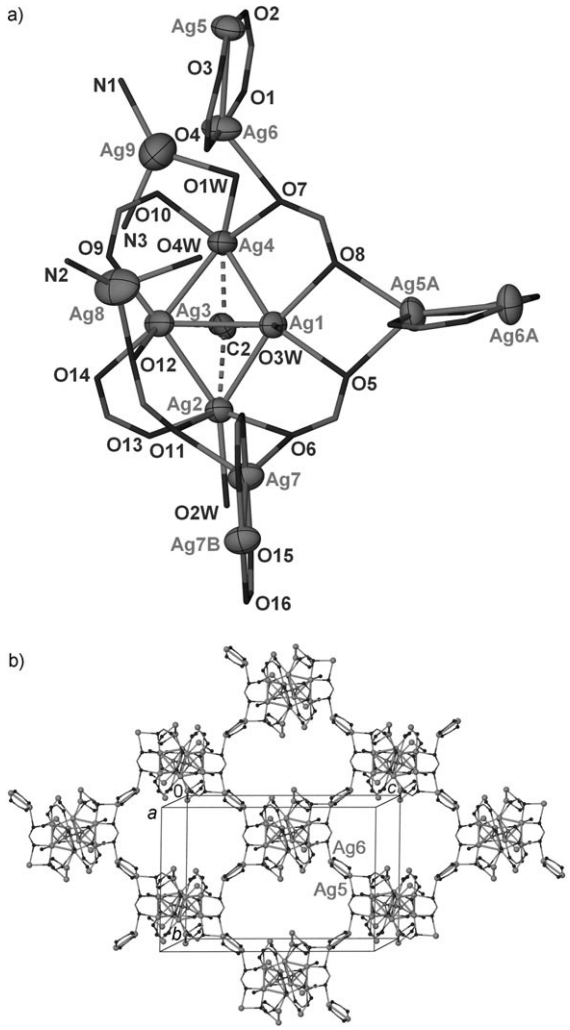

Figure 13. a) Atom labeling (50% thermal ellipsoids) and coordination modes of the anionic and neutral ligands in $Ag_2C_4{\cdot}16\,AgC_2F_5CO_2{\cdot}6\,CH_3CN{\cdot}8\,H_2O$ (**7**). All C_2F_5 moieties are omitted for clarity. Symmetry codes: A: $^1/_2-x$, $y-^1/_2$, $1^1/_2-z$; B: $-x$, $-y$, $1-z$. Selected bond lengths and distances (Å): C1–C2 1.22 (1), Ag···Ag 2.845(1)–3.081(1). b) (4,4) Coordination network parallel to the *bc* plane with each $[Ag_4C_4Ag_4]$ aggregate connected by four $[Ag_2(\mu_2\text{-}C_2F_5CO_2)_2]$ bridging units. All C_2F_5 moieties and other ligands are omitted for clarity.

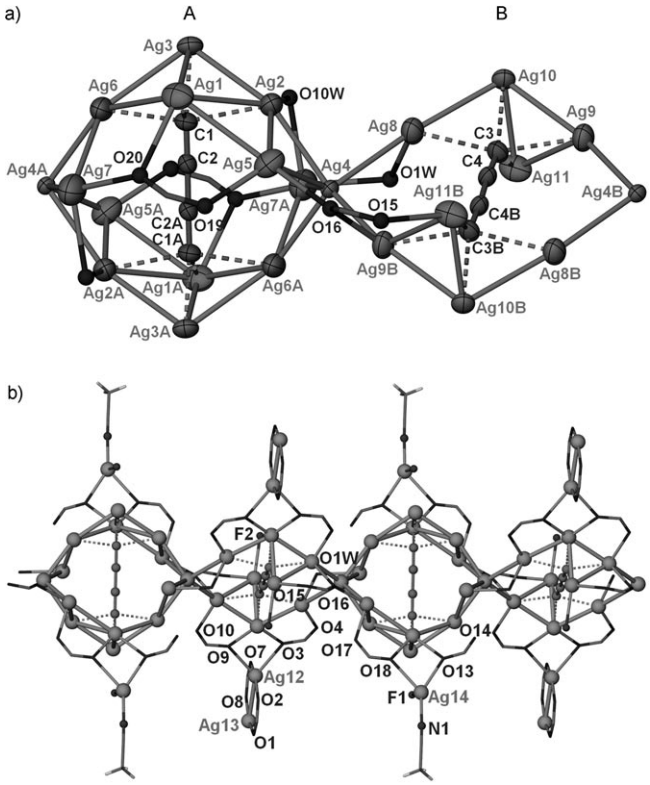

Figure 14. a) Atom labeling (50% thermal ellipsoids) in $Ag_2C_4{\cdot}2\,AgF{\cdot}10\,AgC_2F_5CO_2{\cdot}CH_3CN{\cdot}12\,H_2O$ (**8**), which contains two metallacycles (A and B). Other groups are omitted for clarity. Symmetry codes: A: $1-x$, $1-y$, $1-z$; B: $1-x$, $2-y$, $1-z$. Selected bond lengths (Å): C1–C2 1.23(1), C3–C4 1.22(1). b) Adjacent metallacycles in **8** connected by sharing the silver atom Ag4 and further bridged by the trifluoroacetate group O15–O16 and the aqua ligand O1W. All C_2F_5 moieties are omitted for clarity.

with a mean deviation of 0.187 Å, and the bond lengths between neighboring silver atoms lie in the range 2.884(1) to 3.023(1) Å with Ag–Ag–Ag angles of 99.21(3)–108.84(4)° for vertex atoms and 153.54(4)–167.22(4)° for atoms between the vertices. Four silver atoms (Ag2, Ag3, Ag4, and Ag6) and those related by inversion together constitute the core eight-membered ring of the silver metallacycle A. These atoms are also coplanar with a mean deviation of 0.253 Å. This plane forms an angle of 47.7° with the mean plane of ring B, whereas the angle between the two C_4 chains is 73.2°. Thus, the C_4 chains are not coplanar with the corresponding eight-membered rings. The lengths of the eight Ag···Ag edges in the metallacycle lie between 2.844(1) and 3.005(3) Å, and the bond angles lie in the range 106.25(6)–107.87(6)° at Ag3 and Ag4 and 150.1(1)–156.95(5)° at Ag2 and Ag6. Six silver atoms (Ag1, Ag5, Ag7, and the inversion-related atoms) lie above and below this eight-membered ring to form an Ag_{14} girdle, which is consolidated by two pentafluoropropionate groups of the type O19–O20 and two aqua ligands of the type O10W. The Ag_{10} and Ag_{14} silver segments are fused alternately by sharing silver atoms of the type Ag4 to generate a silver column along the *b* direction. One pentafluoropropionate group (O15–O16) and an aqua ligand (O1W) also bridge the two segments (Figure 14b). Notably, the bridging unit $[Ag_2(\mu\text{-}C_2F_5CO_2)_2]$ composed of silver atoms (Ag12 and Ag13) and $C_2F_5CO_2^-$ groups (O1–O2 and O7–O8) is not involved in the connection between silver columns as a result of long Ag–O bonds of 2.63 Å in length.

The addition of $AgBF_4$ increases the concentration of silver ions when aqueous solutions of less water-soluble silver salts, such as $AgCF_3CO_2$, $AgC_2F_5CO_2$, and $AgCF_3SO_3$, are used to dissolve the polymeric compound Ag_2C_2.[29] However, the tetrafluoroborate ions can undergo hydrolysis to yield F^- and such species as $BF_3(OH)^-$ and $BF_2(OH)_2^-$.[19a,30] The existence of two independent fluoride ligands in **8** can be rationalized by the fact that the charge balance is satisfied, and that the Ag–F bond lengths be-

tween the silver atoms Ag14 and Ag11 and fluoride ligands F1 and F2 of 2.404(8) and 2.406(9) Å, respectively, are significantly shorter than the Ag–O bonds between aqua ligands and silver atoms (2.459(8)–2.588(9) Å). Thus, F1 acts as a terminal ligand bonded to the external silver atom Ag14, but F2 together with the abundant water molecules of crystallization construct an intricate hydrogen-bonded system to link adjacent silver columns further to form a 2D network.

As shown in Figure 15, nine independent water molecules and F2 together with the inversion-related species form a series of five- and six-membered rings through hydrogen bonding. Two water molecules (O3W and O11W), one coordinated water molecule (O9W), and the inversion-related molecules form a chairlike cyclic $(H_2O)_6$ hexamer in which the O···O hydrogen-bonding distances lie between 2.802 and 2.887 Å and the O···O···O angles for O3W and O11W are 134.9° and 101.3°, respectively. In contrast, the O···O···O angle at silver-bonded O9W is just 86.1°. This chair conformation similar to that found in the structure of ice occurs commonly in crystalline hydrates.[31] A five-membered hydrogen-bonded ring formed by four water molecules and one fluoride ligand adopts an envelope-like configuration with O3W lying out of the basal plane. The O···O(F) distances between the atoms in the ring are in the range 2.746–2.866 Å. Another six-membered ring consists of a planar arrangement of four water molecules (O4W, O5W, O8W, and O12W) and one fluoride ligand (F2) with a mean deviation from the plane of 0.052 Å, and one silver-bonded water molecule (O7W) that lies above this plane. This configurational diversity relative to the aforementioned chairlike $(H_2O)_6$ cluster may be attributed to the participation of the fluoride ligand in hydrogen bonding. The O···O(F) distances in the six-membered ring range from 2.695 to 2.842 Å with bond angles of 107.1–129.8°. The geometrical parameters of this $(F)_2(H_2O)_{18}$ hydrogen-bonding tape, which can be described as T6(2)5(4)6(4)5(4)6(2) (T = tape; the numbers in parentheses represent water molecules shared between the adjacent rings) according to the nomenclature introduced by Mascal et al.,[32] are summarized in the Supporting Information. This hydrogen-bonding tape is further connected to 14 carboxylate moieties above and below the silver rings of type B to generate a 2D network (Figure 16).

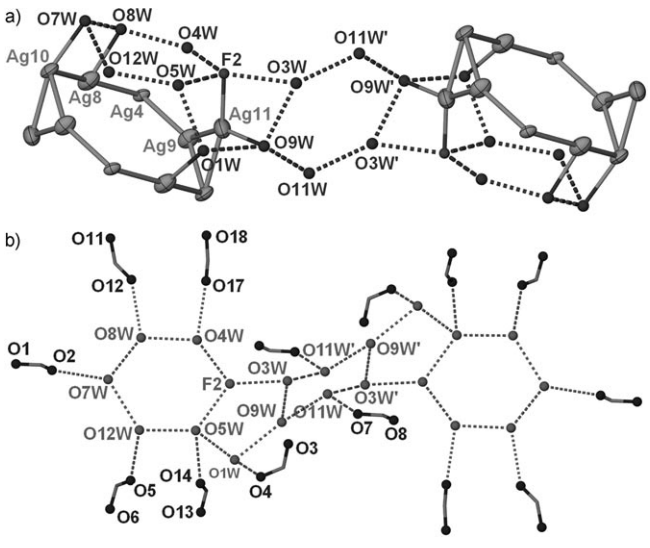

Figure 15. a) Hydrogen-bonding tape T6(2)5(4)6(4)5(4)6(2) of 18 water molecules and two fluoride ligands between two silver metallacycles in $Ag_2C_4{\cdot}2\,AgF{\cdot}10\,AgC_2F_5CO_2{\cdot}CH_3CN{\cdot}12\,H_2O$ (**8**). Other ligands are omitted for clarity. b) Hydrogen bonds between the T6(2)5(4)6(4)5(4)6(2) tape and surrounding pentafluoropropionate groups.

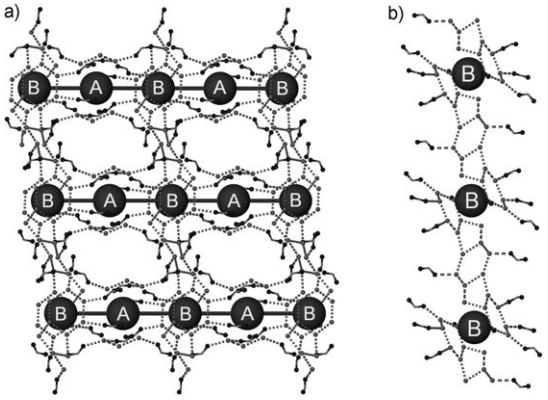

Figure 16. 2D hydrogen-bonding network in **8** with the T6(2)5(4)6(4)5(4)6(2) tape linking the metallacycles of type B.

$Ag_2C_4{\cdot}12\,AgC_2F_5CO_2{\cdot}6\,CH_3CH_2CN{\cdot}4\,H_2O$ (9) and $Ag_2C_4{\cdot}12\,AgC_2F_5CO_2{\cdot}6\,(CH_3)_3CCN{\cdot}5\,H_2O$ (10)

To explore the effect of neutral nitrile ligands, we replaced the acetonitrile added in the preparation of **7** with propionitrile and trimethylacetonitrile, and obtained the two isostructural complexes $Ag_2C_4{\cdot}12\,AgC_2F_5CO_2{\cdot}6\,CH_3CH_2CN{\cdot}4\,H_2O$ (**9**) and $Ag_2C_4{\cdot}12\,AgC_2F_5CO_2{\cdot}6\,(CH_3)_3CCN{\cdot}5\,H_2O$ (**10**), respectively. In the crystal structures of **9** and **10**, each C_4^{2-} ligand is located at an inversion center with the terminal ethynide moieties embraced by butterfly-shaped Ag_4 baskets through silver–ethynide interactions in the range 2.128(11)–2.388(11) Å and 2.182(14)–2.412(13) Å, respectively. The two terminal Ag_4 baskets, each of which is connected to the silver atom Ag5 by an Ag···Ag interaction, are bridged by two inversion-related pentafluoropropionate groups through the μ_3-O,O,O′ coordination mode to produce a ten-membered metallacycle (Figure 17a). Another μ_3-$C_2F_5CO_2$ group spans an Ag···Ag edge and also coordinates to an external silver atom, Ag7, which is bonded to a CH_3CH_2CN or $(CH_3)_3CCN$ group (Figure 17b). Furthermore, two pentafluoropropionate groups (O3–O4 and O7–O8) each span an Ag···Ag edge and both connect with an $[Ag_2(\mu_2\text{-}C_2F_5CO_2)_2]$ unit composed of two silver atoms of the type Ag6 and two inversion-related μ_2 pentafluoropropionate groups of the type O5–O6 (Figure 17b). An Ag6–O4 bond length of 2.590(9) Å and an Ag6–O7 bond length of 2.519(10) Å were observed for **9**,

CHEMISTRY
AN ASIAN JOURNAL

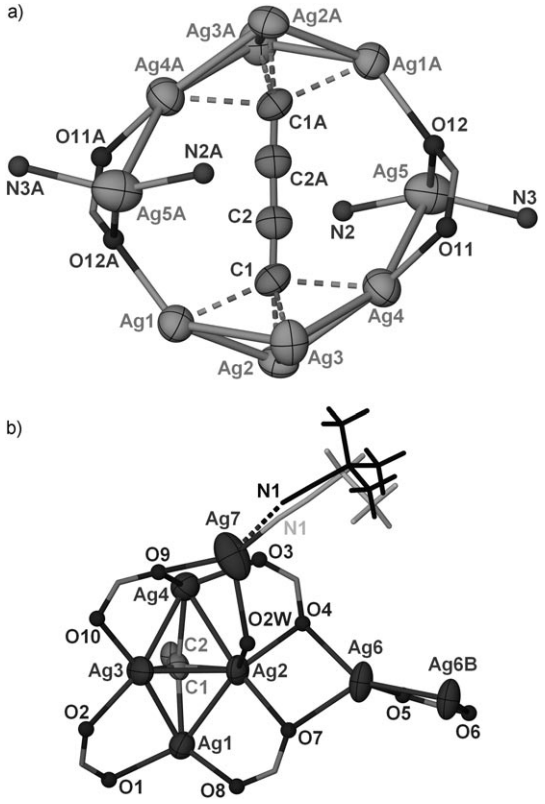

Figure 17. a) Atom labeling (50% thermal ellipsoids) in $Ag_2C_4{\cdot}12\,AgC_2F_5CO_2{\cdot}6\,CH_3CH_2CN{\cdot}4\,H_2O$ (**9**) and the isostructural complex $Ag_2C_4{\cdot}12\,AgC_2F_5CO_2{\cdot}6\,(CH_3)_3CCN{\cdot}5\,H_2O$ (**10**), which contain a 10-membered metallacycle. b) Coordination skeleton of the terminal ethynide moiety of the C_4^{2-} ligand in **9** and **10**. All C_2F_5 moieties are omitted for clarity. The propionitrile group bonded to Ag7 in **9** and the trimethylacetonitrile group bonded to Ag7 in **10** are in gray and black, respectively. Symmetry codes: A: $1-x$, $-y$, $1-z$; B: $1-x$, $-y$, $-z$. Selected bond lengths and distances (Å): **9**: C1–C2 1.26(1), Ag···Ag 2.803(1)–3.204(2); **10**: C1–C2 1.19(2), Ag···Ag 2.872(2)–3.318(2).

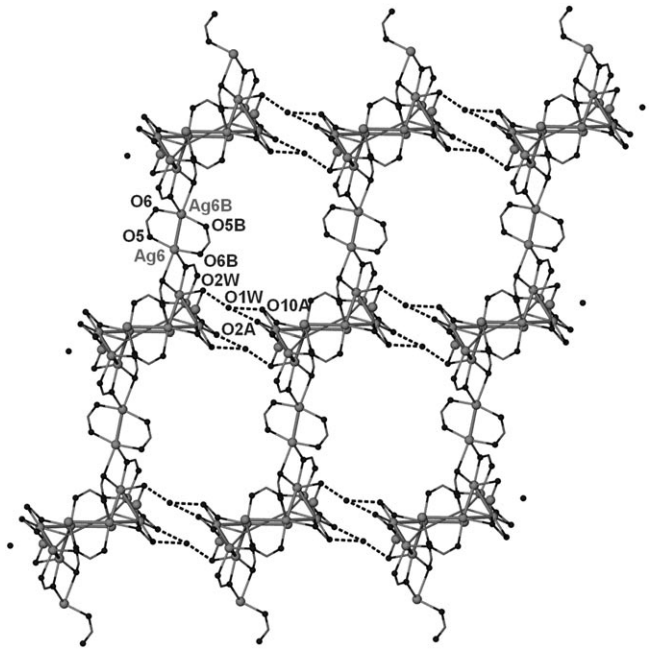

Figure 18. 2D (4,4) network in **9** and **10** linked by $[Ag_2(\mu_2\text{-}C_2F_5CO_2)_2]$ units along the *c* direction and bridged by three hydrogen bonds along the *a* direction. All C_2F_5 moieties and nitrile groups are omitted for clarity. Selected distances (Å): **9**: O1W···O2W 2.719, O1W···O2A 2.887, O1W···O10A 2.970; **10**: O1W···O2W 2.694, O2W···O2A 2.852, O2W···O10A 2.970. Symmetry codes: A: $2-x$, $-y$, $1-z$; B: $1-x$, $-y$, $-z$.

and corresponding bond lengths of 2.649 and 2.576(12) Å were found for **10**. Adjacent ten-membered metallacycles are linked by this bridging unit along the *c* direction to generate a coordination chain, which is further connected by three hydrogen bonds to yield a 2D network parallel to the *ac* plane (Figure 18). The bulky nitrile ligand in **10** enlarges the separation between adjacent (4,4) networks from 12.881 Å in **9** to 13.485 Å. The extra water molecule (O3W) in the stoichiometric formula of **10** is accommodated in the interlayer region.

$Ag_2C_4{\cdot}16\,AgC_2F_5CO_2{\cdot}4\,(CH_3)_3CCN{\cdot}6\,H_2O$ (11)

Next, we investigated the effect of varying the molar ratio of Ag_2C_4 to carboxylate ligands on the coordination network and dimensionality. As the solubility of polymeric Ag_2C_4 depends on the concentration of silver ions, we kept the latter constant but changed the molar ratio $AgC_2F_5CO_2/AgBF_4$ from 1:2 to 2:1, which resulted in the formation of $Ag_2C_4{\cdot}16\,AgC_2F_5CO_2{\cdot}4\,(CH_3)_3CCN{\cdot}6\,H_2O$ (**11**). The centrosymmetric μ_8 coordination mode of C_4^{2-} also exists in the crystal structure of **11**: Each terminus is capped by an Ag_4 basket through σ-type silver–ethynide interactions that range from 2.172(7) to 2.375(7) Å and a π bond between Ag9 and C2 of 2.615(7) Å in length. Each of two silver atoms of the type Ag6 bonds to a terminal Ag_4 aggregate to produce an Ag_5 basket, and these baskets are further bridged by two pentafluoropropionate groups (O7–O8 and O7A–O8A) to generate a 12-membered metallacycle (Figure 19).

Moreover, the pentafluoropropionate group O7–O8 is also connected through the μ_4-O,O′,O′,O′ bonding mode to an external silver atom, Ag7, which is in turn bonded to one trimethylacetonitrile group and an $[Ag_2(\mu_3\text{-}C_2F_5CO_2)]$ bridging unit composed of Ag4 and the pentafluoropropionate group O15–O16. Another μ_4 pentafluoropropionate group, O5–O6, spans one Ag···Ag edge and is connected to the two external silver atoms Ag7 and Ag8. However, the pentafluoropropionate group O1–O2 not only bonds to one Ag···Ag edge, but also bridges two $[Ag_2(C_2F_5CO_2)_2]$ linking units. The linkage of $[Ag_5C_4Ag_5]$ aggregates by these $[Ag_2(C_2F_5CO_2)_2]$ units, which comprise two Ag5 atoms and two O13–O14 pentafluoropropionate groups along the *c* direction and two Ag4 atoms and two O15–O16 pentafluoropropionate groups along the *b* direction, produces a 2D coordination network (Figure 20). This network contrasts strongly with the (4,4) network observed for **9** and **10** with the participation of hydrogen bonding.

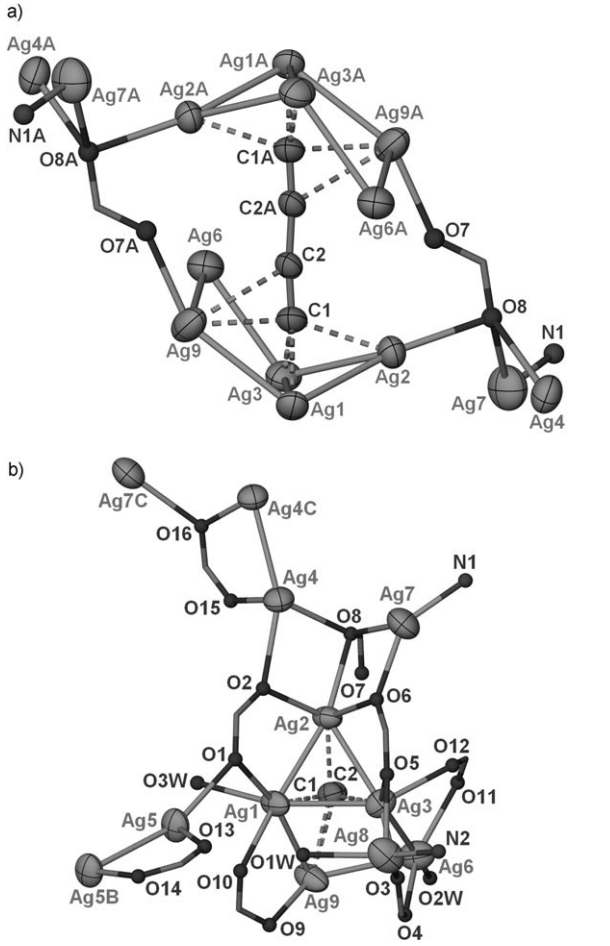

Figure 19. a) Atom labeling (50% thermal ellipsoids) in $Ag_2C_4{\cdot}16\,AgC_2F_5CO_2{\cdot}4\,(CH_3)_3CCN{\cdot}6\,H_2O$ (**11**), which contains a 12-membered metallacycle. b) Coordination configuration of the anionic ligands in **11**. All C_2F_5 moieties, *tert*-butyl groups, and other ligands are omitted for clarity. Symmetry codes: A: $1-x$, $1-y$, $1-z$; B: $1-x$, $1-y$, $-z$; C: $1-x$, $2-y$, $1-z$. Selected bond lengths and distances (Å): C1–C2 1.214(9), Ag···Ag 2.823(1)–3.001(5).

$Ag_2C_4{\cdot}8\,AgC_2F_5CO_2{\cdot}2\,[(Et_4N)C_2F_5CO_2]{\cdot}4\,H_2O$ (12)

In the crystal structure of $Ag_2C_4{\cdot}8\,AgC_2F_5CO_2{\cdot}2\,[(Et_4N)C_2F_5CO_2]{\cdot}4\,H_2O$ (**12**), the centrosymmetric C_4^{2-} dianion is encapsulated in a metallacycle that consists of two Ag_5 aggregates bridged by two pentafluoropropionate groups (O3–O4 and O3A–O4A) and two aqua ligands (O2W and O2WA; Figure 21a).

Versatile coordination modes are observed for the carboxylate ligands in this structure (Figure 21b). Each of two pentafluoropropionate groups (O1–O2 and O7–O8) coordinates with an Ag···Ag edge of the Ag_5 basket through the μ_2-O,O′ mode. The carboxylate ligand O9–O10, however, chelates with the silver atom Ag5. The more complex coordination modes μ_4-O,O,O′,O′ and μ_3-O,O′,O′ are observed for O3–O4 and O5–O6, respectively, which link the $[Ag_5C_4Ag_5]$ units to form a coordination column along the *c* direction. Such coordination columns are further stabilized by a series of hydrogen bonds between O2, O10, O1W, and the aqua ligand

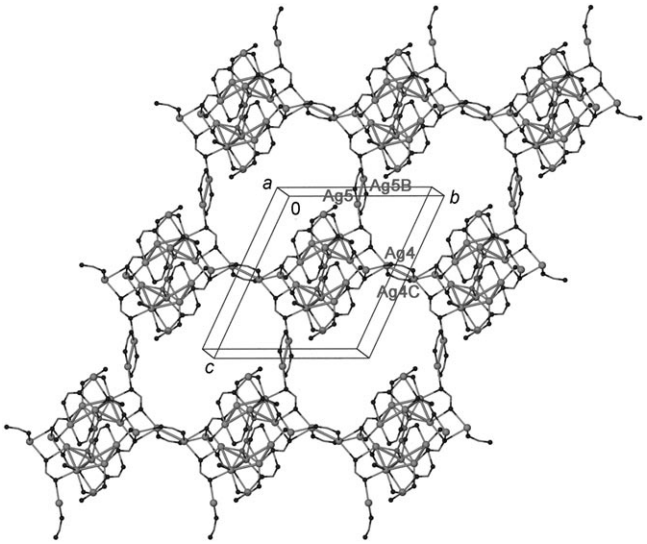

Figure 20. (4,4) Coordination network in **11** oriented parallel to the *bc* plane and bridged by two types of $[Ag_2(C_2F_5CO_2)_2]$ units. All C_2F_5 moieties and other ligands are omitted for clarity. Symmetry codes: B: $1-x$, $1-y$, $-z$; C: $1-x$, $2-y$, $1-z$.

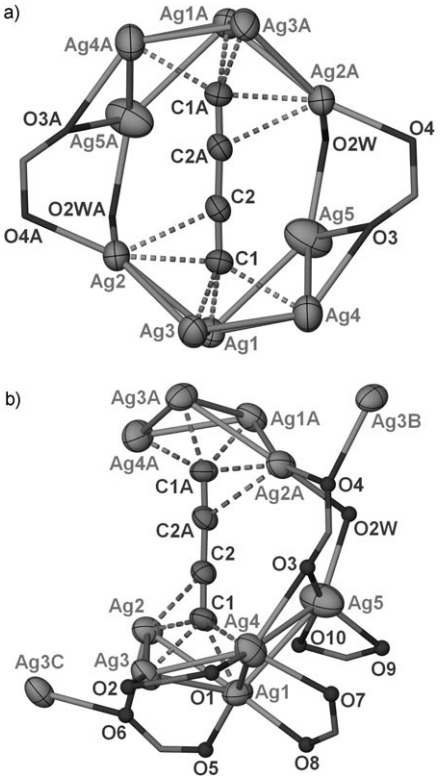

Figure 21. a) Perspective view of the metallacycle in $Ag_2C_4{\cdot}8\,AgC_2F_5CO_2{\cdot}2\,[(Et_4N)C_2F_5CO_2]{\cdot}4\,H_2O$ (**12**) formed through the linkage of two terminal Ag_5 baskets by pentafluoropropionate groups (O3–O4 and O3A–O4A) and aqua ligands (O2W and O2WA), with atom labeling (50% thermal ellipsoids). b) Coordination modes of pentafluoropropionate groups in **12**. All C_2F_5 moieties and other peripheral ligands are omitted for clarity. Symmetry codes: A: $-x$, y, $^1/_2-z$; B: x, $1-y$, $z-^1/_2$; C: $-x$, $1-y$, $1-z$. Selected bond lengths and distances (Å): C1–C2 1.22(1), Ag···Ag 2.857(1)–3.198(2).

CHEMISTRY
AN ASIAN JOURNAL

O2W (Figure 22a) and are arranged in a hexagonal array with the tetraethylammonium cations located in the interstices (Figure 22b).

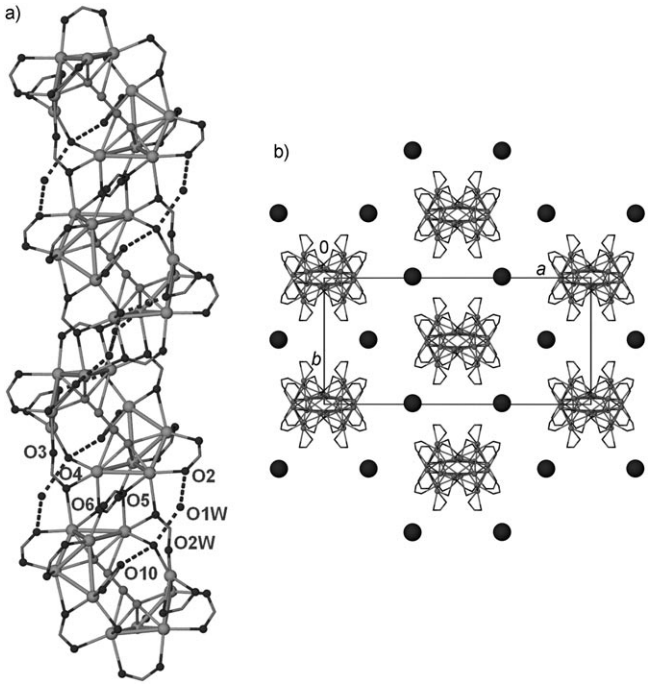

Figure 22. a) Coordination column in **12** connected by two independent pentafluoropropionate groups (O3–O4 and O5–O6) and surrounded by a series of hydrogen-bonding straps. All C_2F_5 moieties are omitted for clarity. Selected distances (Å): O1W···O2 2.856, O1W···O2W 2.741, O2W···O10 2.719. b) Hexagonal array of coordination columns in **12** viewed along the *c* direction. The tetraethylammonium cations (represented by large black spheres) occupy the interstices between the columns. All C_2F_5 moieties are omitted for clarity.

$3\,Ag_2C_4{\cdot}12\,AgC_2F_5CO_2{\cdot}5\,[(BnMe_3N)C_2F_5CO_2]{\cdot}4\,H_2O$ (13)

The presence of the bulky ammonium cation $BnMe_3N^+$ (Bn = benzyl), induces the sharing of silver atoms by the supramolecular synthon $Ag_4{\subset}C{\equiv}C{-}C{\equiv}C{\supset}Ag_4$ and thus leads to the formation of a novel $Ag_9{\subset}(C_4)_3{\supset}Ag_9$ cluster aggregate in the crystal structure of $3\,Ag_2C_4{\cdot}12\,AgC_2F_5CO_2{\cdot}5\,[(BnMe_3N)C_2F_5CO_2]{\cdot}4\,H_2O$ (**13**). As shown in Figure 23a, three 1,3-butadiynediide ligands are embraced by two nearly planar Ag_9 segments, which are bridged by four pentafluoropropionate groups through the μ_3-O,O′,O′ bonding mode. The C_4 chains have a mean twist angle of 49° and all adopt the μ_8 coordination mode, with each terminus bonded to four silver atoms (Figure 23a). The two Ag_9 segments have a similar configuration despite different Ag···Ag distances, and each side can be described as three $C{\equiv}C{\supset}Ag_4$ moieties that share three central silver atoms and are consolidated by other pentafluoropropionate groups that span the Ag···Ag edges. Moreover, these two similar Ag_9 segments are almost parallel to one another with a dihedral angle of 3.7°, and a quasi-C_3 axis passes through the centers of the Ag1···Ag4···Ag7 and Ag10···Ag13···Ag16 triangles (Figure 23b). Thus, this $Ag_9{\subset}(C_4)_3{\supset}Ag_9$ aggregate has quasi-D_3 symmetry.

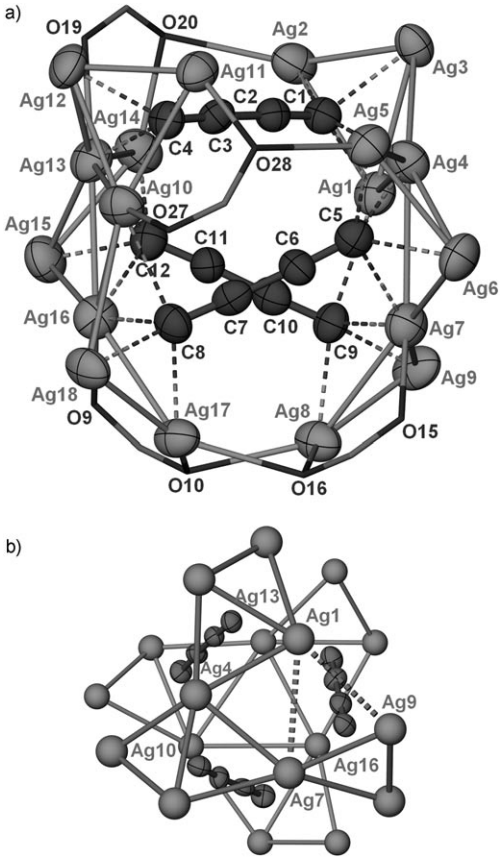

Figure 23. a) Perspective view of the $Ag_9{\subset}(C_4)_3{\supset}Ag_9$ aggregate in $3\,Ag_2C_4{\cdot}12\,AgC_2F_5CO_2{\cdot}5\,[(BnMe_3N)C_2F_5CO_2]{\cdot}4\,H_2O$ (**13**), in which two parallel planar Ag_9 segments are bridged by four μ_3-O,O,O′ pentafluoropropionate groups, with atom labeling (40% thermal ellipsoids). The C_2F_5 moieties and other ligands are omitted for clarity. Selected bond lengths (Å): C1–C2 1.22(2), C3–C4 1.24(2), C5–C6 1.21(2), C7–C8 1.22(2), C9–C10 1.23(1), C11–C12 1.22(1). b) $Ag_9{\subset}(C_4)_3{\supset}Ag_9$ aggregate viewed along the vector from the center of the triangle Ag1–Ag4–Ag7 to the center of the triangle Ag10–Ag13–Ag16 to show its quasi-D_3 symmetry. The Ag···Ag distances shown by solid lines range from 2.812(1) to 3.328(1) Å and are thus shorter than twice the van der Waals radius of a silver ion (3.4 Å). The longer Ag···Ag edges are represented by dashed lines (Å): Ag1···Ag7 3.506, Ag1···Ag9 3.462.

Furthermore, adjacent $Ag_9{\subset}(C_4)_3{\supset}Ag_9$ aggregates surrounded by pentafluoropropionate groups are linked by an aqua ligand O2W along the *b* direction to generate a zigzag coordination column (Figure 24). These coordination columns are arranged in a hexagonal array similar to that observed for **12**, and the $BnMe_3N^+$ ions are located in the interstices.

The $[Ag_4C_4Ag_4]$ Aggregate

The invariable appearance of the μ_8 bonding mode of the 1,3-butadiynediide ligand in reported silver(I) double salts $Ag_2C_4{\cdot}6\,AgNO_3{\cdot}n\,H_2O$ ($n = 2$, 3) and the present 13 complexes substantiates our presumption that the $Ag_4{\subset}C{\equiv}C{-}$

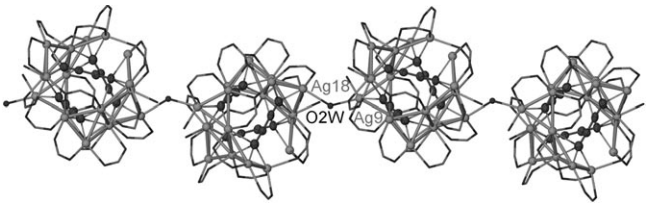

Figure 24. Coordination column in **13** along the *b* direction bridged by the aqua ligand O2W. Quaternary ammonium cations are omitted for clarity.

C≡C⊃Ag_4 moiety can serve as a new type of supramolecular synthon in the construction of coordination networks of variable dimensions. However, the configuration of the Ag_4 aggregate that embraces each ethynide terminus can be fine-tuned by varying the coexisting anionic or neutral ligands to give a butterfly-shaped, planar, or barblike geometry. These different Ag_4 configurations may be ascribed to diverse silver–ethynide interactions that play different roles in the μ_8 coordination modes, which can be broadly classified into three types: σ, π, and mixed (σ,π). The crystallographic data for the [$Ag_4C_4Ag_4$] aggregates in complexes **1**–**13** are summarized in the Supporting Information. We classify the silver–ethynide interactions in these complexes according to the Ag–C bond lengths and C≡C–Ag bond angles. The σ-type Ag–C bonds are much shorter than the other two bond types, and the corresponding C≡C–Ag bond angles are close to 180° (Table 2). In contrast, the significantly longer π-type Ag–C bonds are accompanied by acute C≡C–Ag bond angles, which is consistent with the picture of a silver(I) atom that interacts with a pair of linked sp-hybridized carbon atoms. Bonds of the mixed (σ,π) type correspond to silver–ethynide bonding for which the bond lengths and angles lie between these two extremes. The three different Ag_4 configurations observed in the present study can be considered to arise from various combinations of the three types of Ag–C interactions: The barblike Ag_4 aggregate in **1** can be described as [σ×1+(σ,π)×3], the planar Ag_4 aggregate in **3** as [σ×2+π×2], another aggregate in **6** as [σ×4], and the butterfly-shaped aggregate as [σ×2+(σ,π)×2] or [σ×2+π×1+(σ,π)×1]. Furthermore, most Ag···Ag distances in this series of 13 silver complexes of Ag_2C_4 are shorter than 3.40 Å (twice the van der Waals radius of the silver atom), which indicates that a significant argentophilic interaction[16] plays a pivotal role in the formation of the [$Ag_4C_4Ag_4$] aggregates.

Anionic Ligands

By analogy with Ag_2C_2,[33] when polymeric Ag_2C_4 is dissolved in a concentrated aqueous medium that contains silver(I) ions, the labile $[C_4@Ag_8]^{6+}$ species thus formed need to be neutralized and stabilized by anionic ligands during the crystallization process. Thus, the presence of one or more ancillary anionic ligands is a key factor in the supramolecular assembly of the Ag_4⊂C≡C–C≡C⊃Ag_4 synthon in

Table 2. Classification of the silver–ethynide interactions in the silver 1,3-butadiynediide complexes **1**–**13**.

Complex	$Ag_4C_4Ag_4$ type	Type of bonding	C2–Ag [Å]	C1–Ag [Å]	C1≡C2–Ag [°]
1	butterfly	σ×2	2.128(5)–2.151(5)		137.5(4)–140.0(4)
		π×1	2.519(7)	2.667(7)	83.0(4)
		(σ,π)×1	2.423(6)		106.3(4)
	barb	σ×1	2.067(6)		178.8(5)
		(σ,π)×3	2.347(6)–2.508(6)		93.5(4)–97.1(4)
2	butterfly	σ×2	2.134(16)–2.295(15)		124.8(11)–155.5(11)
		π×1	2.368(16)–2.401(16)	2.718–2.737	91.2(10)–93.0(13)
		(σ,π)×1	2.315(15)–2.393(15)		100.7(14)–105.0(11)
3	butterfly	σ×2	2.156(19)–2.183(19)		136.7(15)–139.0(15)
		(σ,π)×2	2.287(19)–2.360(19)		101.8(13)–104.5(13)
	planar	σ×2	2.18(2)–2.20(2)		136.4(18)-143.1(18)
		π×2	2.31(2)–2.58(2)	2.52(2)–2.60(2)	77.2(14)-85.6(15)
4	butterfly	σ×3	2.186(6)–2.277(7)		120.2(5)–143.1(5)
		π×1	2.440(6)–2.483(7)	2.548(5)–2.721	80.6(4)–87.7(4)
5	butterfly	σ×2	2.226(7)–2.238(7)		140.0(6)–141.3(6)
		(σ,π)×2	2.361(8)–2.378(8)		104.6(6)–106.1(6)
6	planar	σ×4	2.206(12)		123.4(6)
7	butterfly	σ×2	2.171(9)–2.216(9)		121.7(7)–148.7(7)
		(σ,π)×2	2.290(9)–2.443(9)		98.2(6)–113.8(6)
8	butterfly	σ×2	2.139(9)–2.174(9)		126.8(8)–150.1(9)
		π×1	2.443(9)	2.724	89.8(6)
		(σ,π)×1	2.404(9)–2.423(10)		101.5(7)–106.9(7)
9	butterfly	σ×2	2.128(11)–2.180(11)		135.9(9)–138.7(9)
		(σ,π)×2	2.326(11)–2.388(11)		91.5(8)–116.7(9)
10	butterfly	σ×2	2.182(14)–2.218(14)		133.7(11)–143.3(11)
		(σ,π)×2	2.411(13)–2.412(13)		97.1(10)-114.5(11)
11	butterfly	σ×2	2.172(7)–2.183(7)		133.4(6)–142.6(6)
		π×1	2.375(7)	2.615(7)	87.3(5)
		(σ, π)×1	2.337(7)		112.0(5)
12	butterfly	σ×2	2.193(10)–2.209(10)		136.1(8)–136.2(9)
		π×1	2.379(10)	2.579(9)	85.1(7)
		(σ, π)×1	2.356(10)		121.5(8)
13	butterfly	σ×2	2.169(12)–2.259(12)		132.2(9)–142.0(10)
		(σ, π)×2	2.275(11)–2.695(12)		92.2(8)–117.5(9)
		σ×2	2.148(11)–2.256(12)		127.2(9)–145.5(10)
		π×1	2.526(11)–2.699(12)	2.764–2.841	83.5(8)–89.1(8)

Table 2. (Continued)

Complex	$Ag_4C_4Ag_4$ type	Type of bonding	C2−Ag [Å]	C1−Ag [Å]	C1≡C2−Ag [°]
		(σ,π)×1	2.296(11)–2.316(12)		108.6(8)–111.4(9)

the construction of coordination networks. On the basis of our previous synthesis of the double salts $Ag_2C_4{\cdot}6\,AgNO_3{\cdot}n\,H_2O$ ($n=2$, 3), we used silver nitrate together with silver fluoride to obtain the triple salt **1**, which has a similar robust 3D-coordination-network structure. The second known quadruple salt **2** was acquired through the hydrolysis of PF_6^-. The coordination columns of **2** are linked by a series of nitrate and phosphate groups to yield a 3D coordination network. However, when carboxylate ligands with a hydrophobic tail ($CF_3CO_2^-$ and $C_2F_5CO_2^-$) were employed, relatively loose 3D coordination networks were obtained, as observed for **3** and **6**, the melting points of which are much lower than those of the four nitrate complexes. The formation of loose coordination networks and porous crystal structures may be due to the steric effects of the carboxylate ligands and their weak coordination ability relative to that of the nitrate group. Moreover, a comparison of **10** and **11** demonstrates that the dimensionality of the coordination network can be modulated by varying the molar ratio of anionic ligands in the preparation of the complexes.

Nitrile Ligands

In the present study, nitrile ligands of varying sizes were often introduced to effect crystallization. Apparently, when nitrile ligands participate in the crystallization process, they bond to a peripheral silver atom and prevent sterically the linkage of carboxylate ligands to form higher-dimensional coordination networks. This behavior accounts for the variation in the trifluoroacetate complexes **3**, **4**, and **5**, and in the pentafluoropropionate complexes **7**, **9**, **10**, and **11**. Thus, the use of nitrile ligands of varying degrees of bulkiness provides an efficacious approach to the design of low-dimensional coordination networks.

Quaternary Ammonium Salts

Quaternary ammonium ions have been utilized effectively in the generation of a vast variety of inclusion compounds, in which they serve as guest species for charge balance and space filling.[34] In the complexes described herein, such cations act to some extent as bulky spheroidal balloons to prevent the self-assembly of high-dimensional networks; thus, a 2D network is observed for **5** and an infinite coordination column for **12**. Furthermore, the use of quaternary ammonium salts as additional components necessarily leads to the formation of various types of anionic silver(I) coordination columns and 2D and 3D networks in which more-anionic ligands are bound to the metal centers and/or the fusion of aggregates is facilitated. As a result of the combined steric effects of $C_2F_5CO_2^-$ and the bulky ammonium cation $BnMe_3N^+$, the supramolecular synthon $Ag_4C_4Ag_4$ is apt to share silver atoms, thus leading to the formation of the novel $Ag_9{\subset}(C_4)_3{\supset}Ag_9$ aggregate in **13**.

Conclusions

We have investigated systematically the synthesis and structure of a series of 13 silver(I) complexes of Ag_2C_4 (Table 3). The generation of the quadruple salt **2** by the hydrolysis of hexafluorophosphate represents a viable route to multiple salts for future studies. Diverse configurations of the $[Ag_4C_4Ag_4]$ aggregate were observed in which C_4^{2-} was found to adopt the μ_8 bonding mode consistently. These configurations can be tuned by varying the ancillary anionic ligands. The silver–ethynide interactions in the aggregates can be classified conveniently into three types: σ, π, and mixed (σ,π). We also investigated the effects of various types of coexisting nitrile ligands to obtain a better understanding for the design of other coordination networks with the $Ag_4{\subset}C{\equiv}C{-}C{\equiv}C{\supset}Ag_4$ supramolecular synthon. The $(F)_2(H_2O)_{18}$ fluoride–water tape in **8** and the $(C_4)_3@Ag_{18}$ aggregate in **13** are both unprecedented among silver(I) complexes.

Experimental Section

Reagents and Instruments

Hexachloro-1,3-butadiene (97%, Aldrich), 1,4-bis(trimethylsilyl)-1,3-butadiyne (98%, International Laboratory), and *n*BuLi in hexane (1.6 M, Merck) were purchased and used without further purification. Tetrahydrofuran (THF) was purified by heating at reflux over metallic sodium and benzophenone. All other reagents were of analytical grade and used as received. Infrared spectra were obtained from KBr pellets on a Nicolet Impact 420 FTIR spectrometer in the 400–4000-cm^{-1} region. Elemental analysis (C, H, N) was performed by the Medac Ltd. Brunel Science Center, United Kingdom.

Syntheses

Method A for the preparation of Ag_2C_4: As described previously,[11] the treatment of Li_2C_4 (generated in situ from hexachloro-1,3-butadiene and *n*BuLi) with solid $AgNO_3$ in a 1:2 molar ratio in THF yielded a 1:1 mixture of Ag_2C_4 (≈40%) and AgCl (≈50 wt%) contaminated with a minute amount of metallic silver as a dark-gray powder.

Method B for the preparation of Ag_2C_4: THF (20 mL) was cooled to −78 °C in a 100-mL Schlenk flask, and *n*BuLi in hexane (1.6 M, 5.1 mL, 8.2 mmol) was added with a syringe. The mixture was stirred for 15 min at −78 °C, and then a solution of 1,4-bis(trimethylsilyl)-1,3-butadiyne (0.778 g, 4 mmol) in THF (5 mL) was added dropwise with a syringe. The cold bath was then removed, and the mixture was stirred at room temperature for 3 h. THF (10 mL) and $AgNO_3$ crystals (1.352 g, 8 mmol) were added to the flask under a stream of nitrogen. The solid $AgNO_3$ dissolved gradually, and the mixture was stirred overnight. Ag_2C_4 (78%) contaminated with a small amount of metallic silver was isolated by filtration as a light-gray powder, then washed several times with THF and finally with deionized water.

Caution: Ag_2C_4 should be stored wet in the dark at −10 °C, and only a small quantity should be used for subsequent synthesis.

1: Moist Ag_2C_4 (0.2 g) was added to a concentrated aqueous solution of $AgNO_3$ (1 mL; 0.513 g, 3 mmol) in a beaker, and the mixture was stirred

until the solution was saturated. The excess Ag_2C_4 was filtered off, and the filtrate was mixed with an aqueous solution of AgF (1 mL; 0.370 g, 3 mmol). The resulting mixture was placed in the dark. After 1 day, the transparent yellow blocklike crystals of **1** (≈40%) that had deposited were collected. Compound **1** turns black above 110 °C. M.p. (decomp.): 125.5–127.1 °C; IR: $\tilde{\nu}=2060\ cm^{-1}$ (vw, ν(C≡C)); elemental analysis: calcd (%) for $C_8H_2F_2O_{19}N_6Ag_{12}$: C 5.28, H 0.11, N 4.62; found: C 5.10, H 0.27, N 4.31.

2: $AgNO_3$ (0.342 g, 2 mmol) and $AgPF_6$ (0.253 g, 1 mmol) were dissolved in deionized water (1 mL). Moist Ag_2C_4 (0.2 g) was added to the solution, and the resulting mixture was stirred for about half an hour then filtered. The filtrate was placed in the dark at room temperature. After a few days, yellow prismatic crystals of **2** (≈30%) were collected. Compound **2** decomposes above 170 °C. IR: $\tilde{\nu}=2050\ cm^{-1}$ (vw, ν(C≡C)); elemental analysis: calcd (%) for $C_4F_2O_{18}N_4P_2Ag_{10}$: C 3.06, N 3.57; found: C 2.88, N, 3.21.

3: Moist Ag_2C_4 (≈0.2 g) was added to a concentrated aqueous solution (1 mL) of $AgCF_3CO_2$ (0.234 g, 1 mmol) and $AgBF_4$ (0.380 g, 2 mmol) in a beaker, and the mixture was stirred until the solution was saturated. The excess Ag_2C_4 was filtered off, and the solution was placed in a refrigerator at −10 °C. After a few days, the transparent yellow blocklike crystals of **3** (≈40%) that had deposited were collected. M.p. (decomp.): 70.3–71.6 °C; IR: $\tilde{\nu}=2056\ cm^{-1}$ (m, ν(C≡C)); elemental analysis: calcd (%) for $C_{16}H_{14}F_{18}O_{19}Ag_8$: C 11.20, H 0.82; found: C 11.09, H 0.77.

4: A synthetic procedure similar to that for the preparation of **3** was used, but CH_3CN (0.1 mL) was added to the filtrate before it was placed in a refrigerator at −10 °C. Pale-yellow blocklike crystals of **4** (≈30%) were deposited. M.p.: 67.3–69.0 °C; IR: $\tilde{\nu}=2064\ cm^{-1}$ (vw, ν(C≡C)); elemental analysis: calcd (%) for $C_{20}H_{11}F_{21}O_{18}NAg_9$: C 12.49, H 0.58, N 0.73; found: C 12.33, H 0.67, N 0.58.

5: Ag_2C_4 (≈0.2 g) and solid $(Et_4N)BF_4$ (0.1 g) were added to a concentrated aqueous solution (1 mL) of $AgCF_3CO_2$ (0.220 g, 1 mmol) and $AgBF_4$ (0.382 g, 2 mmol) in a beaker, and the mixture was stirred until the solution was saturated. The excess Ag_2C_4 and $(Et_4N)BF_4$ were filtered off, and $(CH_3)_3CCN$ (0.1 mL) was added to the filtrate, which was then placed in a refrigerator at −10 °C. After a few days, the transparent pale-yellow platelike crystals of **5** (≈30%) that had deposited were collected. M.p.: 62.3–64.0 °C; IR: 2055 cm^{-1} (vw, ν(C≡C); elemental analysis: calcd (%) for $C_{64}H_{76}F_{36}O_{24}N_6Ag_{12}$: C 23.35, H 2.33, N 2.55; found: C 23.26, H 2.34, N 2.25.

Table 3. Crystallographic data for compounds **1**–**13**.

Compound	**1**	**2**	**3**	**4**	**5**	**6**	**7**
Formula	$C_8H_2F_2O_{19}N_6Ag_{12}$	$C_4F_2O_{18}N_4P_2Ag_{10}$	$C_{16}H_{14}F_{18}O_{19}Ag_8$	$C_{20}H_{11}F_{21}O_{18}NAg_9$	$C_{64}H_{76}F_{36}O_{24}N_6Ag_{12}$	$C_{52}H_{50}F_{80}O_{56}Ag_{16}$	$C_{64}H_{34}F_{80}O_{40}N_6Ag_{18}$
M_r	1818.54	1570.72	1715.18	1923.07	3291.67	4816.66	4988.45
Crystal system	monoclinic	monoclinic	orthorhombic	monoclinic	monoclinic	tetragonal	monoclinic
Space group	*C*2/*c* (No. 15)	$P2_1$ (No. 4)	$P2_12_12_1$ (No. 19)	*C*2/*c* (No. 15)	$P2_1/n$ (No. 14)	$P4_2/nmc$ (No.137)	*C*2/*c* (No. 15)
a [Å]	23.312(1)	6.623(1)	14.246(4)	32.366(5)	17.768(5)	18.696(1)	30.343(5)
b [Å]	10.663(1)	16.678(2)	23.445(7)	11.730(2)	16.063(4)	18.696(1)	17.745(3)
c [Å]	13.167(1)	10.159(1)	11.670(4)	26.827(4)	17.804(5)	18.495(1)	27.272(4)
α [°]	90	90	90	90	90	90	90
β [°]	124.168(1)	93.941(2)	90	123.638(3)	91.772(7)	90	111.327(5)
γ [°]	90	90	90	90	90	90	90
V [Å^3]	2708.0(2)	1119.5(2)	3898(2)	8479(2)	5079(2)	6464.9(6)	13678(4)
Z	4	2	4	8	2	2	4
D_c [g cm^{-3}]	4.456	4.660	2.899	3.000	2.126	2.481	2.415
T [K]	293	293	293	293	293	293	293
μ [mm^{-1}]	8.575	8.796	4.085	4.223	2.388	2.562	2.689
$R1$[a] ($I>2\sigma$)	0.0245	0.0455	0.0863	0.0414	0.0497	0.0756	0.0585
$wR2$[b] (all data)	0.0624	0.1280	0.2146	0.1223	0.1109	0.2727	0.1703
GOF	1.059	1.081	1.106	1.026	1.064	1.088	0.999

Compound	**8**	**9**	**10**	**11**	**12**	**13**
Formula	$C_{36}H_{27}F_{52}O_{32}NAg_{14}$	$C_{58}H_{38}F_{60}O_{28}N_6Ag_{14}$	$C_{70}H_{64}F_{60}O_{29}N_6Ag_{14}$	$C_{72}H_{48}F_{80}O_{38}N_4Ag_{18}$	$C_{50}H_{48}F_{50}O_{24}N_2Ag_{10}$	$C_{113}H_{88}F_{85}O_{38}N_5Ag_{18}$
M_r	3483.64	3916.99	4103.33	5038.64	3089.51	5680.40
Crystal system	triclinic	monoclinic	monoclinic	triclinic	monoclinic	monoclinic
Space group	$P\bar{1}$ (No. 2)	$P2_1/n$ (No. 14)	$P2_1/n$ (No. 14)	$P\bar{1}$ (No. 2)	*C*2/*c* (No. 15)	$P2_1/c$ (No. 14)
a [Å]	16.377(3)	13.490(2)	14.369(3)	15.663(1)	35.539(4)	18.542(2)
b [Å]	16.699(3)	25.763(4)	26.970(5)	15.803(1)	15.288(2)	25.200(3)
c [Å]	19.318(4)	16.551(3)	16.943(3)	17.424(1)	18.077(2)	35.713(4)
α [°]	115.495(4)	90	90	111.402(1)	90	90
β [°]	111.796(4)	109.874(6)	111.775(4)	97.449(1)	114.750(2)	91.311(3)
γ [°]	90.599(4)	90	90	112.345(1)	90	90
V [Å^3]	4336(2)	5409(2)	6097(2)	3528.9(4)	8920(2)	16682(3)
Z	2	2	2	1	4	4
D_c [g cm^{-3}]	2.650	2.400	2.230	2.365	2.295	2.223
T [K]	293	293	293	293	293	293
μ [mm^{-1}]	3.266	2.641	2.350	2.606	2.314	2.222
$R1$[a] ($I>2\sigma$)	0.0591	0.0619	0.0814	0.0470	0.0714	0.0664
$wR2$[b] (all data)	0.1720	0.1478	0.2260	0.1405	0.2268	0.2278
GOF	0.959	1.056	1.077	1.019	1.077	1.001

[a] $R1=\Sigma||F_o|-|F_c||/\Sigma|F_o|$. [b] $wR2=\{\Sigma[w(F_o^2-F_c^2)^2]/\Sigma[w(F_o^2)^2]\}^{1/2}$.

6: This complex was prepared according to the method used to prepare **3** by adding $AgCF_3CF_2CO_2$ (0.270 g, 1 mmol) in place of $AgCF_3CO_2$. M.p.: 103.6–105.2 °C (decomp. above 122 °C); IR: $\tilde{\nu}=2073\ cm^{-1}$ (vw, ν(C≡C)); elemental analysis: calcd (%) for $C_{52}H_{50}F_{80}O_{56}Ag_{16}$: C 12.97, H 1.05; found: C 12.74, H 1.03.

7: $AgCF_3CF_2CO_2$ (0.270 g, 1 mmol) and $AgBF_4$ (0.382 g, 2 mmol) were dissolved in deionized water (1 mL), and moist solid Ag_2C_4 (≈0.2 g) was added to the solution. The resulting mixture was stirred for 10 min, then the excess Ag_2C_4 was filtered off. CH_3CN (0.1 mL) was added to the filtrate, which was then placed in a refrigerator at −10 °C. After several days, the pale-yellow blocklike crystals of **7** (≈55%) that had deposited were collected. M.p.: 38.2–41.0 °C (decomp. above 128 °C); IR: $\tilde{\nu}=2075\ cm^{-1}$ (vw, ν(C≡C)); elemental analysis: calcd (%) for $C_{64}H_{34}F_{80}O_{40}N_6Ag_{18}$: C 15.41, H 0.69, N 1.68; found: C 15.36, H 0.75, N 1.50.

8: Ag_2C_4 (≈0.2 g) was added to a concentrated aqueous solution (1 mL) of $AgCF_3CF_2CO_2$ (0.542 g, 2 mmol) and $AgBF_4$ (0.190 g, 1 mmol) in a beaker, and the mixture was stirred until the solution was saturated. The excess Ag_2C_4 was filtered off, the filtrate was placed in a desiccator filled with acetonitrile vapor, and the solution was stored in the desiccator in a refrigerator at −10 °C for about 1 month. The transparent pale-yellow blocklike crystals of **8** (≈15%) that had deposited were then collected. Compound **8** decomposes above 125 °C. IR: $\tilde{\nu}=2042\ cm^{-1}$ (vw, ν(C≡C)); elemental analysis: calcd (%) for $C_{36}H_{27}F_{52}O_{32}NAg_{14}$: C 12.42, H 0.78, N 0.40; found: C 12.50, H 0.73, N 0.27.

9: Pale-yellow crystals of **9** (≈35%) were obtained by the procedure used to prepare **7** by adding propionitrile (0.1 mL) in place of acetonitrile. M.p.: 56.3–57.0 °C; IR: $\tilde{\nu}=2062\ cm^{-1}$ (vw, ν(C≡C)); elemental analysis: calcd (%) for $C_{58}H_{38}F_{60}O_{28}N_6Ag_{14}$: C 17.78, H 0.98, N 2.14; found: C 17.45, H 1.14, N 2.07.

10: Pale-yellow blocklike crystals of **10** (≈40%) were obtained by the method used to prepare **7** by adding $(CH_3)_3CCN$ (0.1 mL) in place of acetonitrile. M.p.: 69.2–72.0 °C; IR: $\tilde{\nu}=2083\ cm^{-1}$ (vw, ν(C≡C)); elemental analysis: calcd (%) for $C_{70}H_{64}F_{60}O_{29}N_6Ag_{14}$: C 20.49, H 1.57, N 2.05; found: C 20.33, H 1.35, N 1.98.

11: Yellow blocklike crystals of **11** (≈35%) were obtained by the method used to prepare **10** by changing the molar ratio of $AgCF_3CF_2CO_2$ to $AgBF_4$ from 1:2 to 2:1. M.p.: 75.7–77.0 °C; IR: $\tilde{\nu}=2061\ cm^{-1}$ (vw, ν(C≡C)); elemental analysis: calcd (%) for $C_{72}H_{48}F_{80}O_{38}N_4Ag_{18}$: C 17.16, H 0.96, N 1.11; found: C 17.19, H 0.67, N 0.92.

12: Moist Ag_2C_4 (0.2 g) and solid $(Et_4N)BF_4$ (0.1 g) were added successively to a concentrated aqueous solution (1 mL) of $AgCF_3CF_2CO_2$ (0.542 g, 2 mmol) and $AgBF_4$ (0.190 g, 1 mmol). The mixture was stirred for 0.5 h, then the excess Ag_2C_4 and $(Et_4N)BF_4$ were filtered off, and the filtrate was placed in a refrigerator at −10 °C. After 1 week, transparent pale-yellow prismatic crystals of **12** (≈30%) were collected. M.p.: 62.4–64.1 °C; IR: $\tilde{\nu}=2074\ cm^{-1}$ (vw, ν(C≡C)); elemental analysis: calcd (%) for $C_{50}H_{48}F_{50}O_{24}N_2Ag_{10}$: C 19.44, H 1.56, N 0.91; found: C 19.44, H 1.26, N 0.87.

13: Moist solid Ag_2C_4 (0.2 g) was added to a concentrated aqueous solution (1 mL) of $AgCF_3CF_2CO_2$ (0.542 g, 2 mmol) and $AgBF_4$ (0.190 g, 1 mmol). The mixture was stirred for 0.5 h, then the excess Ag_2C_4 was filtered off. A solution of $(BnMe_3N)BF_4$ (0.5 M) in acetonitrile (0.2 mL) was added to the filtrate, which was then placed in a refrigerator at −10 °C for 2 months. Transparent pale-yellow block crystals of **13** (≈55%) were obtained. M.p.: 63.4–65.0 °C; IR: $\tilde{\nu}=2057\ cm^{-1}$ (vw, ν(C≡C)); elemental analysis: calcd (%) for $C_{113}H_{88}F_{85}O_{38}N_5Ag_{18}$: C 23.89, H 1.56, N 1.23; found: C 23.62, H 1.34, N 1.07.

X-ray Crystallographic Analysis

Data for complexes **1** and **6** were collected at 293 K with $Mo_{K\alpha}$ radiation on a Bruker SMART APEX II CCD diffractometer with frames of oscillation range 0.3°. Intensities for the other 11 complexes were measured on a Bruker SMART 1000 CCD diffractometer by using the same procedure. During data reduction, an empirical absorption correction was applied by using the SADABS program.[35] The structures were solved by direct methods, and non-hydrogen atoms were located from difference Fourier maps. All non-hydrogen atoms, unless otherwise noted, were subjected to anisotropic refinement by full-matrix least-squares on F^2 by using the SHELXTL program.[36] The parameters for the crystal data and X-ray structure analysis are summarized in Table 3. The refinement details are described in the Supporting Information. CCDC-650195–650207 (**1**–**13**, respectively) contain the supplementary crystallographic data for this paper. These data can be obtained free of charge from The Cambridge Crystallographic Data Centre at http://www.ccdc.cam.ac.uk/data_request/cif.

Acknowledgements

We gratefully acknowledge financial support from the Hong Kong Research Grants Council (CERG Ref. No. CUHK 402405) and the Wei Lun Foundation.

[1] a) J. Jortner, M. Ratner, *Molecular Electronics*, Blackwell Science, Oxford, **1997**; b) F. Paul, C. Lapinte, *Coord. Chem. Rev.* **1998**, *178–180*, 431–509; c) R. M. Metzger, *Chem. Rev.* **2003**, *103*, 3803–3834; d) N. Robertson, C. A. McGowan, *Chem. Soc. Rev.* **2003**, *32*, 96–103; e) V. W.-W. Yam, K. M.-C. Wong, *Top. Curr. Chem.* **2005**, *257*, 1–32; f) S. Rigaut, C. Olivier, K. Costuas, S. Choua, O. Fadhel, J. Massue, P. Turek, J. Y. Saillard, P. H. Dixneuf, D. Touchard, *J. Am. Chem. Soc.* **2006**, *128*, 5859–5876.

[2] a) J.-L. Brédas, R. R. Chance, *Conjugated Polymer Materials: Opportunities in Electronic, Optoelectronic and Molecular Electronics*, *Vol. 182*, *NATO ASI Series*, Kluwer, Dordrecht, **1990**; b) T. J. J. Muller, H. J. Lindner, *Chem. Ber.* **1996**, *129*, 607–613; c) H. Nakashini, N. Sumi, S. Ueno, K. Takiyima, Y. Aso, T. Otsubo, K. Komaguchi, M. Shiotani, N. Ohta, *Synth. Met.* **2001**, *119*, 413–414.

[3] a) A. Kraft, A. C. Grimsdale, A. B. Holmes, *Angew. Chem.* **1998**, *110*, 416–443; *Angew. Chem. Int. Ed.* **1998**, *37*, 402–428; b) W. Lu, B.-X. Mi, M. C. W. Chan, Z. Hui, C.-M. Che, N. Zhu, S.-T. Lee, *J. Am. Chem. Soc.* **2004**, *126*, 4958–4971; c) K. M.-C. Wong, X. Zhu, L.-L. Hung, N. Zhu, V. W.-W. Yam, H.-S. Kwok, *Chem. Commun.* **2005**, 2906–2908.

[4] a) N. J. Long, *Angew. Chem.* **1995**, *107*, 37–56; *Angew. Chem. Int. Ed. Engl.* **1995**, *34*, 21–38; b) S. Barlow, D. O'Hare, *Chem. Rev.* **1997**, *97*, 637–669; c) I. R. Whittall, A. M. McDonagh, M. G. Humphrey, *Adv. Organomet. Chem.* **1998**, *42*, 291–362; d) J. Vicente, M. T. Chicote, M. D. Abrisqueta, M. C. Ramirez de Arellano, P. G. Jones, M. G. Humphrey, M. P. Cifuentes, M. Samoc, B. Luther-Davies, *Organometallics* **2000**, *19*, 2968–2974; e) C. E. Powell, M. P. Cifuentes, J. P. Morrall, R. Stranger, M. G. Humphrey, M. Samoc, B. Luther-Davies, G. A. Heath, *J. Am. Chem. Soc.* **2003**, *125*, 602–610; f) M. P. Cifuentes, M. G. Humphrey, *J. Organomet. Chem.* **2004**, *689*, 3968–3981; g) M. P. Cifuentes, M. G. Humphrey, J. P. Morrall, M. Samoc, F. Paul, C. Lapinte, T. Roisnel, *Organometallics* **2005**, *24*, 4280–4288.

[5] a) M. J. Irwin, J. J. Vittal, R. J. Puddephatt, *Organometallics* **1997**, *16*, 3541–3547; b) M. Younus, A. Kohler, S. Cron, N. Chawdhury, M. R. A. Al-Madani, M. S. Khan, N. J. Long, R. H. Friend, P. R. Raithby, *Angew. Chem.* **1998**, *110*, 3180–3183; *Angew. Chem. Int. Ed.* **1998**, *37*, 3036–3039; c) V. W.-W. Yam, K. K.-W. Lo, K. M.-C. Wong, *J. Organomet. Chem.* **1999**, *578*, 3–30; d) V. W.-W. Yam, *Acc. Chem. Res.* **2002**, *35*, 555–563; e) K.-L. Cheung, S.-K. Yip, V. W.-W. Yam, *J. Organomet. Chem.* **2004**, *689*, 4451–4462.

[6] a) S. Lotz, P. H. Van Rooyen, R. Meyer, *Adv. Organomet. Chem.* **1995**, *37*, 219–320; b) N. J. Long, C. K. Williams, *Angew. Chem.* **2003**, *115*, 2690–2722; *Angew. Chem. Int. Ed.* **2003**, *42*, 2586–2617.

[7] a) V. W.-W. Yam, W. K.-M. Fung, K.-K. Cheung, *Angew. Chem.* **1996**, *108*, 1213–1215; *Angew. Chem. Int. Ed. Engl.* **1996**, *35*, 1100–1102; b) C. P. McArdle, J. J. Vittal, R. J. Puddephatt, *Angew. Chem.* **2000**, *112*, 3977–3980; *Angew. Chem. Int. Ed.* **2000**, *39*, 3819–3822; c) V. W.-W. Yam, *Chem. Commun.* **2001**, 789–796; d) V. W.-W. Yam,

J. Organomet. Chem. **2004**, *689*, 1393–1401; e) D. M. P. Mingos, R. Vilar, D. Rais, *J. Organomet. Chem.* **2002**, *641*, 126–133.
[8] a) G.-C. Guo, G.-D. Zhou, T. C. W. Mak, *J. Am. Chem. Soc.* **1999**, *121*, 3136–3141; b) Q.-M. Wang, T. C. W. Mak, *Angew. Chem.* **2002**, *114*, 4309–4311; *Angew. Chem. Int. Ed.* **2002**, *41*, 4135–4137; c) M. I. Bruce, P. J. Low, *Adv. Organomet. Chem.* **2004**, *50*, 179–444, and references therein; d) X.-L. Zhao, Q.-M. Wang, T. C. W. Mak, *Chem. Eur. J.* **2005**, *11*, 2094–2102.
[9] a) J. A. Quet, *C. R. Hebd. Seances Acad. Sci.* **1858**, *46*, 903; b) M. P. Bertholet, *C. R. Hebd. Seances Acad. Sci.* **1860**, *50*, 805; c) J. A. Shaw, E. Fisher, *J. Am. Chem. Soc.* **1946**, *68*, 2745; d) R. Vestin, E. Ralf, *Acta Chem. Scand.* **1949**, *3*, 101–107.
[10] W. Hunsmann, *Chem. Ber.* **1950**, *83*, 213–217.
[11] L. Zhao, T. C. W. Mak, *J. Am. Chem. Soc.* **2004**, *126*, 6852–6853.
[12] a) G. R. Desiraju, *Angew. Chem.* **1995**, *107*, 2541–2558; *Angew. Chem. Int. Ed. Engl.* **1995**, *34*, 2311–2327; b) D. Braga, F. Grepioni, G. R. Desiraju, *Chem. Rev.* **1998**, *98*, 1375–1405; c) G. R. Desiraju, *Acc. Chem. Res.* **2002**, *35*, 565–573.
[13] a) H.-X. Zhang, B.-S. Kang, A.-W. Xu, H.-Q. Liu, Z.-N. Chen, *Comments Inorg. Chem.* **2002**, *23*, 231–248; b) V. Balamurugan, W. Jacob, J. Mukherjee, R. Mukherjee, *CrystEngComm* **2004**, *6*, 396–400; c) J. Burgess, J. R. A. Cottam, P. J. Steel, *Aust. J. Chem.* **2006**, *59*, 295–297.
[14] J.-H. Lee, M. D. Curtis, J. W. Kampf, *Macromolecules* **2000**, *33*, 2136–2144.
[15] a) R. Knorr, *Chem. Rev.* **2004**, *104*, 3795–3849; b) W. A. Chalifoux, R. R. Tykwinski, *Chem. Rec.* **2006**, *6*, 169–182, and references therein.
[16] a) M. Jansen, *Angew. Chem.* **1987**, *99*, 1136–1149; *Angew. Chem. Int. Ed. Engl.* **1987**, *26*, 1098–1110; b) P. Pyykkö, *Chem. Rev.* **1997**, *97*, 597–636; c) M. A. Omary, T. R. Webb, Z. Assefa, G. E. Shankle, H. H. Patterson, *Inorg. Chem.* **1998**, *37*, 1380–1386; d) G.-C. Guo, T. C. W. Mak, *Angew. Chem.* **1998**, *110*, 3296–3299; *Angew. Chem. Int. Ed.* **1998**, *37*, 3183–3186; e) P. Majumdar, K. K. Kamar, S. Goswami, A. Castineiras, *Chem. Commun.* **2001**, 1292–1293; f) L. Pan, E. B. Woodlock, X. Wang, K.-C. Lam, A. L. Rheingold, *Chem. Commun.* **2001**, 1762–1763; g) H.-B. Song, Z.-Z. Zhang, Z. Hui, C.-M. Che, T. C. W. Mak, *Inorg. Chem.* **2002**, *41*, 3146–3154; h) Y. Yoshida, K. Muroi, A. Otsuka, G. Saito, M. Takahashi, T. Yoko, *Inorg. Chem.* **2004**, *43*, 1458–1462; i) X.-D. Chen, M. Du, T. C. W. Mak, *Chem. Commun.* **2005**, 4417–4419.
[17] a) Y.-Y. Lin, S.-W. Lai, C.-M. Che, K.-K. Cheung, Z.-Y. Zhou, *Organometallics* **2002**, *21*, 2275–2282; b) V. W.-W. Yam, W.-Y. Lo, C.-H. Lam, W. K.-M. Fung, K. M.-C. Wong, V. C.-Y. Lau, N. Zhu, *Coord. Chem. Rev.* **2003**, *245*, 39–47; c) V. W.-W. Yam, W.-Y. Lo, N. Zhu, *Chem. Commun.* **2003**, 2446–2447.
[18] a) T. C. Higgs, P. J. Bailey, S. Parsons, P. A. Tasker, *Angew. Chem.* **2002**, *114*, 3164–3167; *Angew. Chem. Int. Ed.* **2002**, *41*, 3038–3041; b) T. C. Higgs, S. Parsons, P. J. Bailey, A. C. Jones, F. McLachlan, A. Parkin, A. Dawson, P. A. Tasker, *Organometallics* **2002**, *21*, 5692–5702.
[19] a) Q.-M. Wang, T. C. W. Mak, *J. Am. Chem. Soc.* **2000**, *122*, 7608–7609; b) P. J. Steel, C. J. Sumby, *Chem. Commun.* **2002**, 322–323.
[20] a) J. C. Jeffery, P. A. Jelliss, V. N. Lebedev, F. G. A. Stone, *Organometallics* **1996**, *15*, 4737–4746; b) R. L. Paul, A. J. Amoroso, P. L. Jones, S. M. Couchman, Z. R. Reeves, L. H. Rees, J. C. Jeffery, J. A. McCleverty, M. D. Ward, *J. Chem. Soc. Dalton Trans.* **1999**, 1563–1568; c) S. Matsukawa, S. Kuwata, Y. Ishii, M. Hidai, *J. Chem. Soc. Dalton Trans.* **2002**, 2737–2746; d) L. Tei, A. J. Blake, P. A. Cooke, C. Caltagirone, F. Demartin, V. Lippolis, F. Morale, C. Wilson, M. Schroeder, *J. Chem. Soc. Dalton Trans.* **2002**, 1662–1670; e) F. Lemaitre, D. Lucas, K. Groison, P. Richard, Y. Mugnier, P. D. Harvey, *J. Am. Chem. Soc.* **2003**, *125*, 5511–5522; f) M. Di Vaira, M. Peruzzini, S. S. Costantini, P. Stoppioni, *J. Organomet. Chem.* **2006**, *691*, 3931–3937; g) D. N. Akbayeva, M. Di Vaira, S. S. Costantini, M. Peruzzini, P. Stoppioni, *Dalton Trans.* **2006**, 389–395.
[21] T. Cargill, M. W. Alexander, D. A. Bardwell, J. C. Jeffery, M. D. Ward, *Inorg. Chim. Acta* **1998**, *267*, 239–247.
[22] a) A. M. Chippindale, S. J. Brech, *Chem. Commun.* **1996**, 2781–2782; b) M.-Y. Lee, S.-L. Wang, *Chem. Mater.* **1999**, *11*, 3588–3594; c) A. A. Ayi, A. Choudhury, S. Natarajan, C. N. R. Rao, *J. Mater. Chem.* **2000**, *10*, 2606–2609; d) Z.-E. Lin, J. Zhang, S.-T. Zheng, G.-Y. Yang, *Z. Anorg. Allg. Chem.* **2005**, *631*, 148–151; e) A. Dakhlaoui, V. Maisonneuve, M. Leblanc, L. S. Smiri, *J. Solid State Chem.* **2005**, *178*, 1880–1887.
[23] a) K. Matsumoto, Y. Sano, M. Kawano, H. Uemura, J. Matsunami, T. Sato, *Bull. Chem. Soc. Jpn.* **1997**, *70*, 1239–1244; b) T. Kuroda-Sowa, M. Munakata, H. Matsuda, S. Akiyama, M. Maekawa, *J. Chem. Soc. Dalton Trans.* **1995**, 2201–2208.
[24] See the Supporting Information and references therein.
[25] Q.-M. Wang, T. C. W. Mak, *J. Am. Chem. Soc.* **2001**, *123*, 1501–1502.
[26] a) M.-L. Tong, S.-L. Zheng, X.-M. Chen, *Chem. Eur. J.* **2000**, *6*, 3729–3738; b) G. A. Bowmaker, J. V. Hanna, C. E. F. Rickard, A. S. Lipton, *J. Chem. Soc. Dalton Trans.* **2001**, 20–28; c) Y.-B. Dong, H.-Y. Wang, J.-P. Ma, D.-Z. Shen, R.-Q. Huang, *Inorg. Chem.* **2005**, *44*, 4679–4692; d) Y.-B. Dong, Y. Geng, J.-P. Ma, R.-Q. Huang, *Organometallics* **2006**, *25*, 447–462.
[27] a) L. Chen, M. A. Khan, G. B. Richter-Addo, *Inorg. Chem.* **1998**, *37*, 533–540; b) A. J. Blake, G. Baum, N. R. Champness, S. S. M. Chung, P. A. Cooke, D. Fenske, A. N. Khlobystov, D. A. Lemenovskii, W.-S. Li, M. Schroder, *J. Chem. Soc. Dalton Trans.* **2000**, 4285–4291; c) S. Camiolo, P. A. Gale, M. E. Light, M. B. Hursthouse, *Supramol. Chem.* **2001**, *13*, 613–618; d) H. Werner, J. Bank, B. Windmuller, O. Gevert, W. Wolfsberger, *Helv. Chim. Acta* **2001**, *84*, 3162–3177; e) C. Archambault, R. Bender, P. Braunstein, Y. Dusausoy, *J. Chem. Soc. Dalton Trans.* **2002**, 4084–4090; f) I. I. R. Salas, M. A. Paz-Sandoval, H. Noth, *Organometallics* **2002**, *21*, 4696–4710; g) J. R. Price, M. Fainerman-Melnikova, R. R. Fenton, K. Gloe, L. F. Lindoy, T. Rambusch, B. W. Skelton, P. Turner, A. H. White, K. Wichmann, *Dalton Trans.* **2004**, 3715–3726.
[28] a) S. A. MacLaughlin, N. J. Taylor, A. J. Carty, *Organometallics* **1983**, *2*, 1194–1202; b) S. Jeannin, Y. Jeannin, F. Robert, C. Rosenberger, *Inorg. Chem.* **1994**, *33*, 243–252; c) A. J. Carty, G. Hogarth, G. Enright, G. Frapper, *Chem. Commun.* **1997**, 1883–1884; d) J. E. Davies, M. J. Mays, P. R. Raithby, K. Sarveswaran, *Angew. Chem.* **1997**, *109*, 2784–2785; *Angew. Chem. Int. Ed. Engl.* **1997**, *36*, 2668–2669; e) T. C. Higgs, S. Parsons, A. C. Jones, P. J. Bailey, P. A. Tasker, *J. Chem. Soc. Dalton Trans.* **2002**, 3427–3428.
[29] Q.-M. Wang, T. C. W. Mak, *Chem. Commun.* **2000**, 1435–1436.
[30] a) J. Reedijk, *Comments Inorg. Chem.* **1982**, *1*, 379–389; b) R. H. Crabtree, G. G. Hlatky, E. M. Holt, *J. Am. Chem. Soc.* **1983**, *105*, 7302–7306; c) P. B. Hitchcock, M. F. Lappert, R. G. Taylor, *J. Chem. Soc. Chem. Commun.* **1984**, 1082–1084; d) D. L. Reger, R. P. Watson, J. R. Gardinier, M. D. Smith, P. J. Pellechia, *Inorg. Chem.* **2006**, *45*, 10088–10097.
[31] a) R. Custelcean, C. Afloroaei, M. Vlassa, M. Polverejan, *Angew. Chem.* **2000**, *112*, 3224–3226; *Angew. Chem. Int. Ed.* **2000**, *39*, 3094–3096; b) J. N. Moorthy, R. Natarajan, P. Venugopalan, *Angew. Chem.* **2002**, *114*, 3567–3570; *Angew. Chem. Int. Ed.* **2002**, *41*, 3417–3420; c) R. J. Doedens, E. Yohannes, M. I. Khan, *Chem. Commun.* **2002**, 62–63; d) B. Venkataramanan, W. L. G. James, J. J. Vittal, V. Suresh, *Cryst. Growth Des.* **2004**, *4*, 553–561; e) B.-Q. Ma, H.-L. Sun, S. Gao, *Chem. Commun.* **2005**, 2336–2338; f) T. K. Prasad, M. V. Rajasekharan, *Cryst. Growth Des.* **2006**, *6*, 488–491; g) M. Estrader, J. Ribas, V. Tangoulis, X. Solans, M. Font-Bardía, M. Maestro, C. Diaz, *Inorg. Chem.* **2006**, *45*, 8239–8250; h) Q.-G. Zhai, C.-Z. Lu, S.-M. Chen, X.-J. Xu, W.-B. Yang, *Inorg. Chem. Commun.* **2006**, *9*, 819–822.
[32] M. Mascal, L. Infantes, J. Chisholm, *Angew. Chem.* **2006**, *118*, 36–41; *Angew. Chem. Int. Ed.* **2006**, *45*, 32–36.
[33] T. C. W. Mak, X.-L. Zhao, Q.-M. Wang, G.-C. Guo, *Coord. Chem. Rev.*, DOI: 10.1016/j.ccr.2006.11.001.
[34] a) T. C. W. Mak, Q. Li in *Advances in Molecular Structure and Research*, *Vol. 4* (Eds.: M. Hargittai, I. Hargittai), JAI Press, Stamford, **1998**, pp. 151–225; b) T. C. W. Mak, F. Xue, *J. Am. Chem. Soc.* **2000**, *122*, 9860–9861; c) C.-K. Lam, T. C. W. Mak, *Angew. Chem.* **2001**,

113, 3561–3563; *Angew. Chem. Int. Ed.* **2001**, *40*, 3453–3455; d) C.-K. Lam, F. Xue, J.-P. Zhang, X.-M. Chen, T. C. W. Mak, *J. Am. Chem. Soc.* **2005**, *127*, 11536–11537.

[35] G. M. Sheldrick, SADABS: Program for Empirical Absorption Correction of Area Detector Data, University of Göttingen, Göttingen (Germany), **1996**.

[36] G. M. Sheldrick, SHELXTL 5.10 for Windows NT: Structure Determination Software Programs, Bruker Analytic X-Ray Systems, Inc., Madison, WI (USA), **1997**.

Received: June 12, 2007
Published online: September 4, 2007

